

# On the water masses and mean circulation of the South Atlantic Ocean

Lothar Stramma

Institut für Meereskunde, Universität Kiel, Kiel, Germany

Matthew England

Center for Environmental Modelling and Prediction, School of Mathematics, University of New South Wales, Sydney, Australia

**Abstract.** We examine recent observations of water mass distribution and circulation schemes at different depths of the South Atlantic Ocean to propose a layered, qualitative representation of the mean distribution of flow in this region. This furthers the simple upper layer geostrophic flow estimates of *Peterson and Stramma* [1991]. In addition, we assess how well ocean general circulation models (GCMs) capture the overall structure of flow in the South Atlantic in this regard. The South Atlantic Central Water (SACW) is of South Atlantic origin in the subtropical gyre, while the SACW in the tropical region in part originates from the South Indian Ocean. The Antarctic Intermediate Water in the South Atlantic originates from a surface region of the circumpolar layer, especially in the northern Drake Passage and the Falkland Current loop, but also receives some water from the Indian Ocean. The subtropical South Atlantic above the North Atlantic Deep Water and north of the Antarctic Circumpolar Current (ACC) is dominated by the anticyclonic subtropical gyre. In the eastern tropical South Atlantic the cyclonic Angola Gyre exists, embedded in a large tropical cyclonic gyre. The equatorial part of the South Atlantic shows several depth-dependent zonal current bands besides the Angola Gyre. Ocean GCMs have difficulty capturing this detailed zonal circulation structure, even at eddy-permitting resolution. The northward extent of the subtropical gyre reduces with increasing depth, located near Brazil at 16°S in the near-surface layer and at 26°S in the Antarctic Intermediate Water layer, while the tropical cyclonic gyre progresses southward. The southward shift of the northern part of the subtropical gyre is well resolved in global ocean GCMs. However, high horizontal resolution is required to capture the South Atlantic Current north of the ACC. The North Atlantic Deep Water in the South Atlantic progresses mainly southward in the Deep Western Boundary Current, but some water also moves southward at the eastern boundary.

## 1. Introduction

During the World Ocean Circulation Experiment (WOCE) many data were collected to get more insight into the South Atlantic Ocean water mass distribution, circulation, and its physical processes. From the large sections carried out during WOCE, information was gained on the water mass distribution and mean circulation, but, in addition, many results from the WOCE data set showed the importance of annual and interannual variability. For example, in TOPEX/POSEIDON data, *Fu* [1996] found the strongest seasonal variability

(both annual and semiannual) in the Brazil/Malvinas Confluence and the Agulhas Retroflexion. From TOPEX/POSEIDON data, *Witter and Gordon* [this issue] described an enhanced, gyre-scale geostrophic circulation in 1993 and 1994, compared with a more sluggish circulation in 1996. To understand the variability, however, first the mean state must be known reasonably well.

Knowledge of the mean South Atlantic subtropical gyre before the intensive WOCE ship surveys began has been summarized by *Peterson and Stramma* [1991], and their upper ocean circulation schematic (their Figure 1) has often been used as a reference for the mean circulation. However, the circulation of the South Atlantic shows some depth dependence and a complicated set of tropical zonal current bands, both unresolved in the flow schematic of *Peterson and Stramma* [1991]. Here

Copyright 1999 by the American Geophysical Union.

Paper number 1999JC900139.

0148-0227/99/1999JC900139\$09.00

we propose and discuss schematic flow fields for three layers of the upper ocean as well as for the Deep Water layer. This is therefore a more detailed and realistic description than the simple one-layer diagram of *Peterson and Stramma* [1991]. We compare the proposed circulation schemes with output from two different global ocean general circulation models (GCMs). Of particular interest is the ability of the models to capture the observed depth-dependent circulation structure in the South Atlantic. The two models differ substantially in horizontal resolution; one is coarse (about  $2^\circ$  resolution), the other is eddy permitting. First, a short description of the water masses will be given, as the schematic diagrams shown represent a specific water mass for large regions, except notably for the southern boundary of the subtropical gyre near  $40^\circ\text{S}$  (where the water mass layers are strongly tilted toward the surface).

## 2. Upper and Deep Ocean Water Masses

In the tropical Atlantic the ocean surface of the South Atlantic is covered by Tropical Surface Water as the surface mixed layer. In the south the surface mixed layer is bounded by the seasonal thermocline. Three major subsurface water masses can be separated for the upper ocean of the tropical and subtropical South Atlantic, while south of the Subantarctic Front near  $45^\circ\text{S}$  (Figure 1a) the ocean is governed by Circumpolar Water (CPW) with quite different T-S characteristics (Figure 1b). In the upper ocean of the tropical and subtropical Atlantic the South Atlantic Central Water (SACW) is observed, which shows a nearly linear T-S relationship (Figure 1b) [*Sverdrup et al.*, 1942]. The SACW is warm and salty compared to the Antarctic Intermediate Water (AAIW) located underneath. In the tropics at about 1000 m depth, Upper Circumpolar Deep Water (UCDW) is the deepest water mass of the upper ocean, with a net northward transport. Below this, North Atlantic Deep Water (NADW) shows a net transport southward. NADW is located underneath Upper Circumpolar Deep Water between about 1200 m in the tropics (1700 m in the subtropics) and 3900 m depth in the tropics (3500 m in the subtropics).

### 2.1. Surface Water

In the surface layer a pool of highly saline water is formed in the tropics/subtropics transition region by subduction [*Tomczak and Godfrey*, 1994] and progresses equatorward and poleward as a subsurface salinity maximum (Figure 1). The strongest formation region in the northwestern South Atlantic is marked in Figure 2. Some very light Subtropical Mode Water at  $16^\circ$  to  $18^\circ\text{C}$  is formed around  $35^\circ\text{S}$  over the Brazil Current [*Provost et al.*, this issue], advected southward and recirculates (Figure 2) slightly below the surface. *Maamaatuaiahutapu et al.* [this issue] observed the formation of this

water during a cruise in September 1994 on a section at  $36.3^\circ\text{S}$  offshore from the Rio de la Plata.

### 2.2. South Atlantic Central Water

The SACW, the water mass south of about  $15^\circ\text{N}$ , shows rather uniform properties throughout its range. Its T-S curve is well described by a straight line between the T-S points  $5^\circ\text{C}$ , 34.3 and  $20^\circ\text{C}$ , 36.0 and is virtually the same as the T-S curves of Indian and Western South Pacific Central Water [*Tomczak and Godfrey*, 1994]. According to *Tomczak and Godfrey* [1994], part of the SACW is not subducted at the Atlantic portion of the subtropical convergence but is, in fact, Indian Central Water (ICW) brought into the Atlantic Ocean by Agulhas Current intrusions. Mixing in the eddy separation region and possibly in the Agulhas Current itself does not change the T-S characteristics of the inflowing ICW but redistributes the contribution of the water types that make up the T-S curve, enhancing, in particular, the volume of water near  $13^\circ\text{C}$ . This water type, also known as  $13^\circ\text{Water}$  [*Tsuchiya*, 1986], thus turns into a variety of Subtropical Mode Water; the associated thermostad can be traced from Namibia to the coast of Brazil near  $10^\circ\text{S}$ , along the North Brazil Current, and into the eastward flowing components of the equatorial current system.

Water masses subducted into the thermocline are commonly known as Central Water. In the formation region during winter a deep surface layer with water of uniform temperature and salinity forms, which is often called Mode Water [e.g., *McCartney*, 1982]. The winter water in the Subantarctic Zone between the Subantarctic Front and the Subtropical Front (Figure 1a) is referred to as Subantarctic Mode Water (SAMW), first discussed by *McCartney* [1977, 1982]. This water is not a water mass but contributes to the Central Water of the Southern Hemisphere [*Tomczak and Godfrey*, 1994]. In the northern part of the Subantarctic Zone a light type of SAMW is located, which actually forms the SACW of the subtropical gyre, while the denser part of the southern Subantarctic Zone is regarded as a precursor of the AAIW. Although the lighter SAMW is only a contribution to the Central Water, it is described in recent literature as a water mass in the subtropical gyre. As the lightest type of Mode Water is formed within the subtropical gyre this is also referred to as Subtropical Mode Water [*Provost et al.*, this issue].

Central Water formation in the South Atlantic does occur in the confluence zone of the Brazil and Falkland Currents (FC) (also often referred to as the Malvinas Current) [*Gordon*, 1981; *Provost et al.*, this issue]. It is responsible for a high-salinity variety of SACW, which recirculates within the southern subtropical gyre (Figure 3). To the south the SACW is bordered by the Subtropical Front at about  $40^\circ\text{S}$  (Figure 1a) connected to the South Atlantic Current [*Stramma and Peterson*, 1990] as the southern boundary of the subtropical gyre.

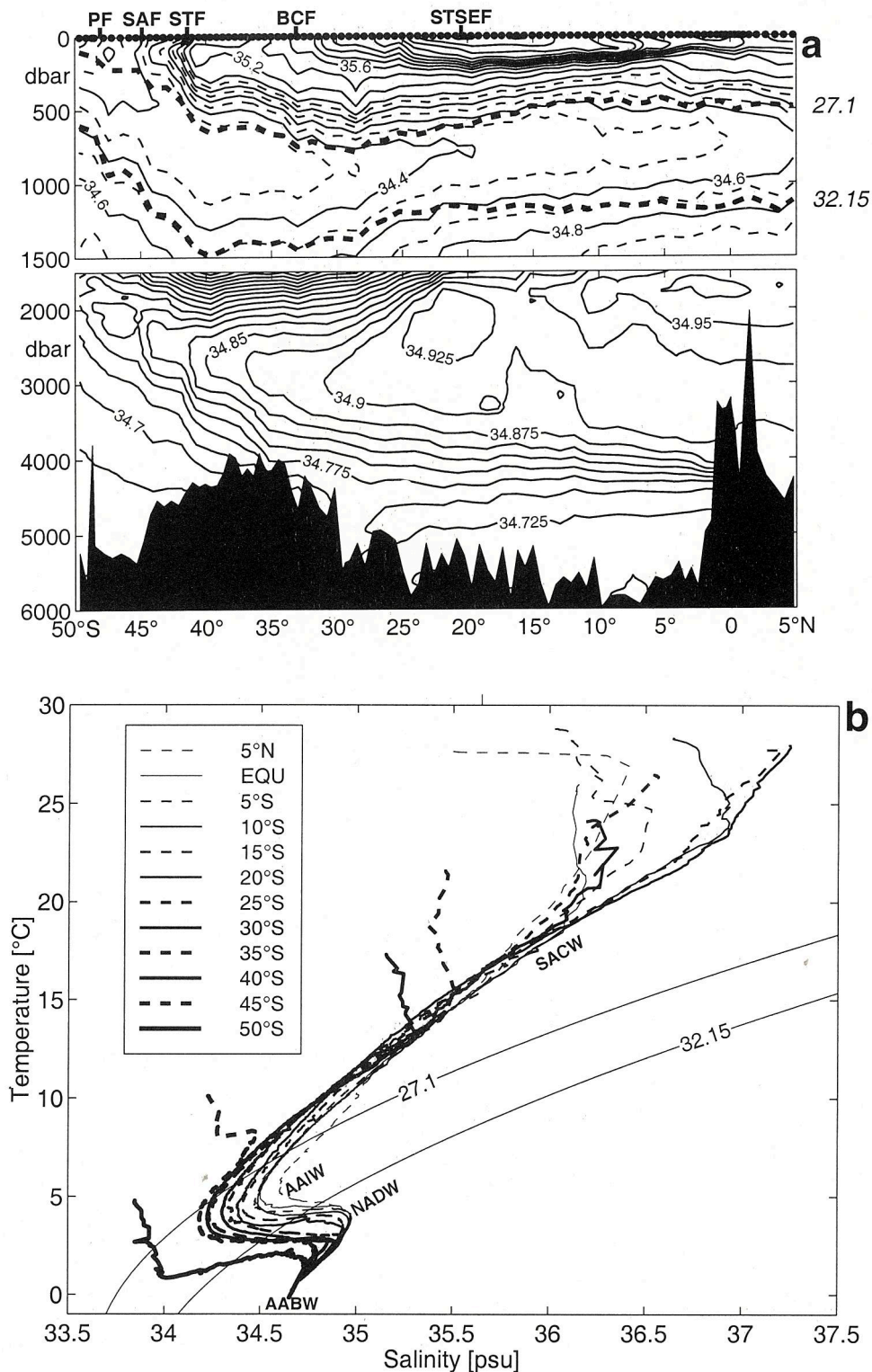


**Figure 1.** (a) Salinity distribution on a meridional section along approximately 25°W from R/V *Melville* in February to April 1989 [Tsuchiya *et al.* 1994], the stations north of the equator are from a R/V *Oceanus* cruise during July to August 1988. The contour interval is 0.2 psu. Within the salinity minimum of the Antarctic Intermediate Water (AAIW) additional 0.1 psu contours are included as dashed lines. The water mass boundaries are indicated by the density surfaces  $\sigma_\theta = 27.1$  and  $\sigma_1 = 32.15$  (thick solid lines). The location of the following fronts [from Talley, 1996] are marked: Polar Front (PF), Subantarctic Front (SAF), Brazil Current Front (BCF), and Subtropical-Subequatorial Front (STSEF). Contour interval for depths greater than 1500 dbar is 0.025. (b) Accompanying T-S diagram showing the changing characteristics of the water masses in 5° latitude steps.

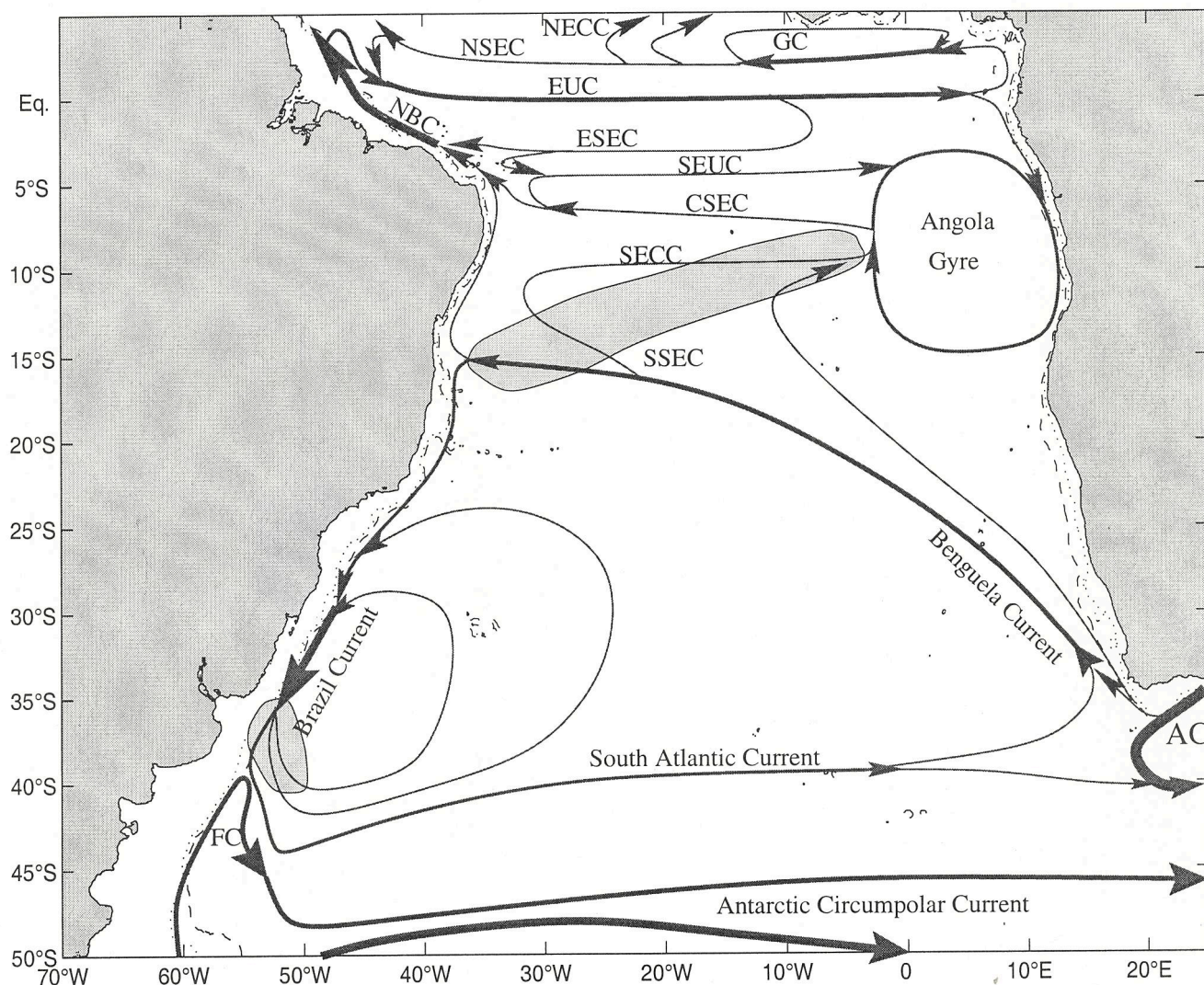


**Figure 2.** Schematic representation of the large-scale, upper 100-m geostrophic currents for southern fall. Shown are the Falkland Current (FC); the Brazil Current; the South Atlantic Current; the Agulhas Current (AC) and its retroflection; the Benguela Current; the South Equatorial Current (SEC), with the northern (NSEC), equatorial (ESEC), central (CSEC), and southern (SSEC) branches; the South Equatorial Countercurrent (SECC); the South Equatorial Undercurrent (SEUC); the Angola Gyre; the Equatorial Undercurrent (EUC); the North Brazil Current (NBC); the North Equatorial Countercurrent (NECC); and the Guinea Current (GC). The topography for 200-m depth is shown as a dotted line and that for 1000-m depth is shown as a short-dashed line. Formation regions of some subsurface water as subsurface salinity maximum water in the tropics and Mode Water in the subtropics are shaded.

Recent observations [e.g., Smythe-Wright *et al.*, 1998] show that the South Atlantic Current is bounded on each side by a distinct front, named the Northern Subtropical Front and the South Subtropical Front. The SACW is transported within the South Atlantic Current toward Africa, where a part contributes directly to the Benguela Current, but part of the SACW passes in the Indian Ocean in a route to the south of the Agulhas Current. The South Atlantic water loops back to the Atlantic within the Indian Ocean, perhaps mostly within the Agulhas recirculation cell of the southwest Indian Ocean [Gordon *et al.*, 1992]. The SACW flows in

the Benguela Current and the South Equatorial Current toward the Brazilian shelf, where it is carried toward the equator with the North Brazil Undercurrent and the North Brazil Current. An oxygen minimum at 300 to 400 m depth is located at the lower limit of the SACW in the tropical regions [e.g., Stramma and Schott, 1996]. The Central Water is of slightly higher salinity north of the equator in the North Atlantic.

### 2.3. Antarctic Intermediate Water

The isopycnals  $\sigma_\theta = 27.1$  (Figure 1) in the tropics and 27.05 in the subtropics mark the transition between

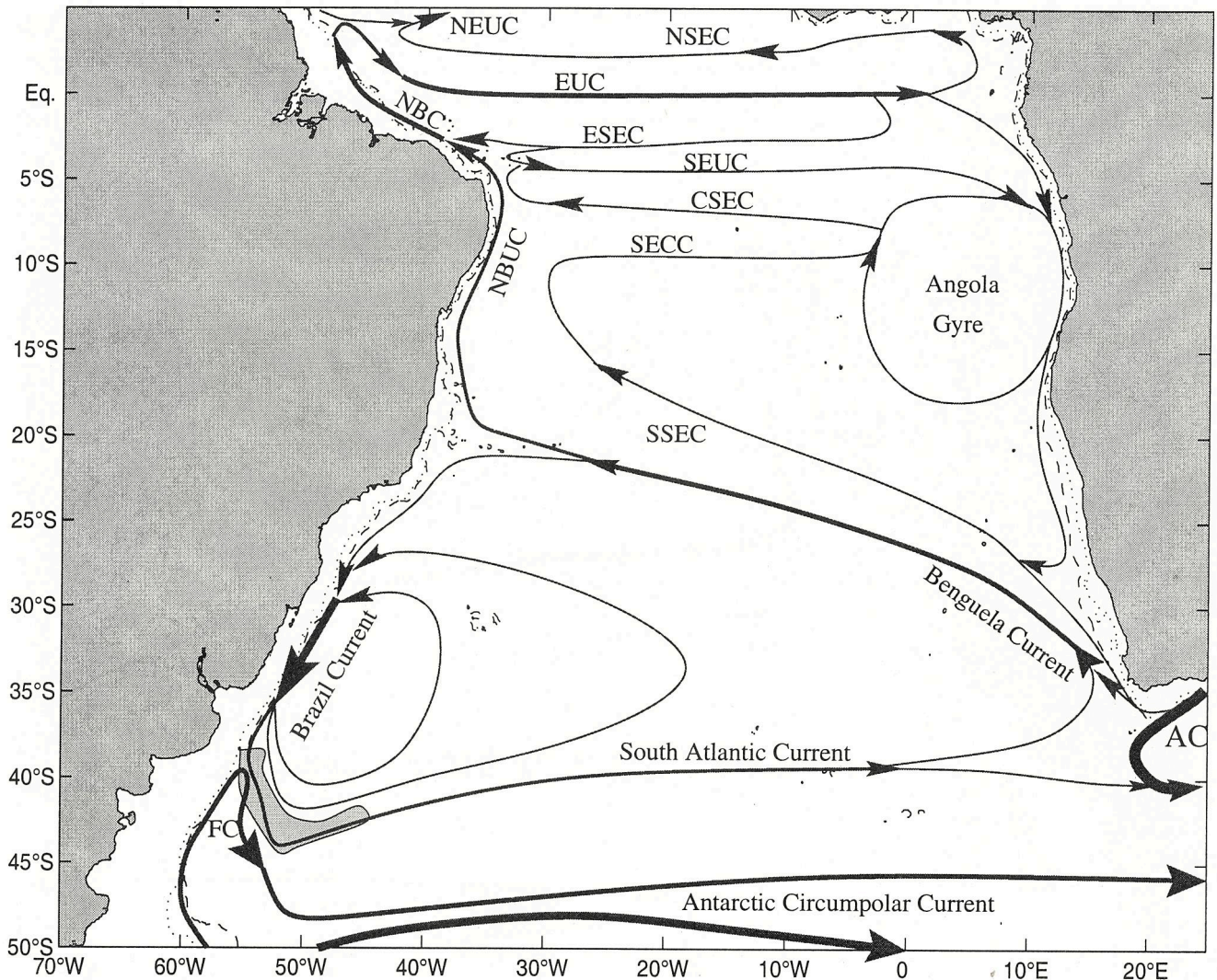


**Figure 3.** Schematic representation of the large-scale, South Atlantic Central Water (SACW) layer (about 100 to 500 m depth) geostrophic currents. Topography and current names are as in Figure 2; in addition, the North Brazil Undercurrent (NBUC) and the North Equatorial Undercurrent (NEUC) are shown. The formation region of this water mass is shaded.

the SACW and the AAIW. *Tsuchiya et al.* [1994] questioned whether the densest SAMW is the direct precursor of AAIW or whether there is substantial input across the Subantarctic Front, while *Maamaatuaiahutapu et al.* [this issue] regard SAMW as the primary precursor of AAIW. The AAIW in the South Atlantic originates from a surface region of the circumpolar layer, especially in the northern Drake Passage and the Falkland Current loop (Figure 4) (and a southern boundary which is essentially the Subantarctic Front [Talley, 1996]). In the east, AAIW from the Indian Ocean is contributed to the South Atlantic AAIW via the Agulhas Current leakage. The AAIW can be recognized by a subsurface oxygen maximum and a salinity minimum (Figure 1) north of about 50°S, although the oxygen maximum becomes weak or absent north of 15°S. *Wüst* [1935] showed an

AAIW oxygen maximum reaching the equator along the western boundary but only to about 20°S in the central and eastern Atlantic. The Subtropical-Subequatorial Front (Figure 1b) marks the northern terminus of the AAIW high-oxygen tongue [Tsuchiya et al., 1994]. The high-oxygen tongue of the AAIW is at a slightly lower density than the salinity minimum. The low-salinity tongue is found at a depth of about 300 m near the Subantarctic Front (45°S), descending northward to 900 m at 30°S in the vicinity of the subtropical gyre center and rising again to 700 m at the equator [Tsuchiya et al., 1994]. A spreading of the AAIW from the South Atlantic to the North Atlantic, identified by a salinity minimum (Figure 1b) near the equator at  $\sigma_\theta$  of about 27.3 [Tsuchiya, 1989] has been described by *Wüst* [1935], who called this water Intermediate Water. The salin-

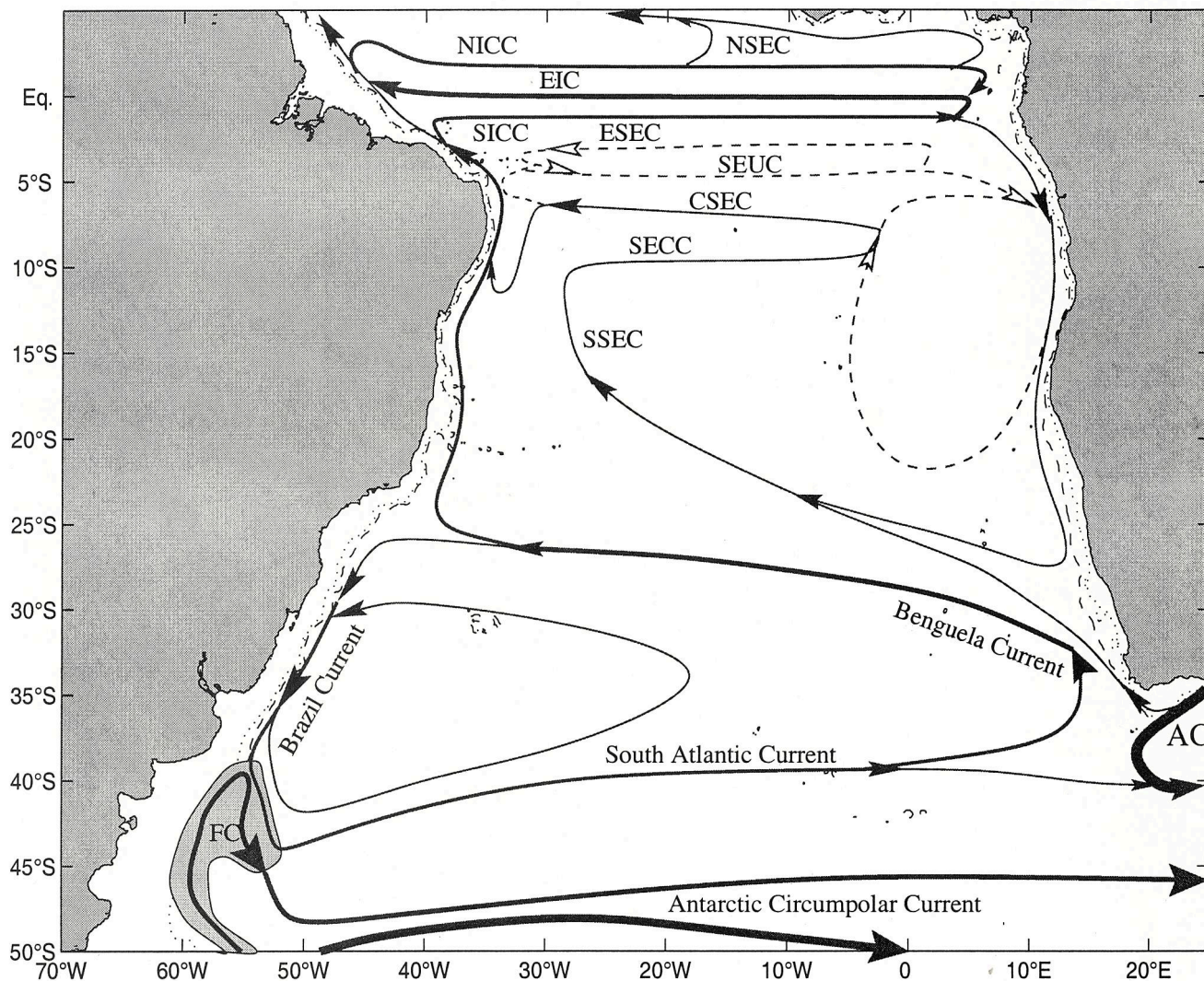


**Figure 4.** Schematic representation of the large-scale, Antarctic Intermediate Water (AAIW) layer (about 500 to 1200 m) geostrophic currents. Topography and current names are as in Figure 2; in addition, the Equatorial Intermediate Current (EIC) and the Northern and Southern Intermediate Countercurrents (NICC and SICC) are shown. The formation region of this water mass is shaded.

ity minimum is present to 24°N [Reid, 1994], although traces of the AAIW can be followed as far north as nearly 60°N [Tsuchiya, 1989].

#### 2.4. Upper Circumpolar Deep Water

Below the AAIW, the northern reaches of the UCDW are found near the equator with phosphate and silica maxima and a temperature minimum at about 1000 m [Reid, 1989]. This water has a source region different from the overlying AAIW, but both water masses flow from the South Atlantic toward the North Atlantic. The CDW is a large body of fresh, oxygen-poor, and nutrient-rich water (compared to the NADW) that flows generally eastward in the Antarctic Circumpolar Current (ACC) and is found over a large density range. In

the Argentine Basin the high-oxygen NADW from the north penetrates into the CPW entering from the Drake Passage and divides it into Upper and Lower Circumpolar Water [Tsuchiya *et al.*, 1994]. An oxygen minimum associated with the UCDW is found in the South Atlantic as a tongue lying below the oxygen maximum of the AAIW and extending northward to about 22°S at 25°W [Tsuchiya *et al.*, 1994]. North of 22°S, the intense, shallow equatorial oxygen minimum obliterates the signature of the UCDW. In the tropics the isopycnal  $\sigma_1 = 32.15$  (Figure 1) separates the UCDW from the North Atlantic Deep Water below; however, in the subtropics the vertical extent of the UCDW increases and the isopycnal  $\sigma_2 = 36.9$  better represents the lower boundary of this water mass [Stramma and Peterson, 1990].

## 2.5. North Atlantic Deep Water

The Deep Western Boundary Current (DWBC) transports North Atlantic Deep Water from the Northern Hemisphere into the South Atlantic. Often, the NADW is separated into three layers as upper, middle, and lower NADW [e.g., *Friedrichs et al.*, 1994], identified by a salinity maximum for the upper NADW and two oxygen maxima for the middle and lower NADW. Using recent WOCE observations near the equator and based on the information of tracer data, *Rhein et al.* [1995] were able to distinguish four different water types within the DWBC. The shallowest part of the upper NADW shows a salinity maximum that is correlated to elevated concentrations of tritium and chlorofluorocarbons (CFCs). This shallow part of the upper NADW was named Shallow Upper NADW (SUNADW) by *Rhein et al.* [1995] or upper Labrador Sea Water (ULSW) by *Pickart* [1992], which is different than the classical LSW. The salinity maximum lies near 1600 m depth near the equator and deepens to 2500 m at 25°S (Figure 1a). However, *Tsuchiya et al.* [1994] suggest from a water mass analysis that the deep salinity maximum south of 25°S is derived from lower NADW and not from upper NADW (or SUNADW), the latter being truncated by the UCDW from the south.

The Labrador Sea Water underneath the SUNADW is formed in the central Labrador Sea, but in the tropics the LSW shows a lower CFC signal than the SUNADW above and is identified by an oxygen maximum. Within the lower NADW (LNADW) a CFC minimum is located above a CFC maximum, and *Rhein et al.* [1995] separated this into (1) old LNADW with a CFC minimum originating from the Charlie Gibbs Fracture Zone Water and (2) overflow NADW (OLNADW) with a CFC maximum and an oxygen maximum originating from the Denmark Strait Overflow Water. The depth range influenced by the NADW varies from about 1200 to 3900 m near the equator and 1700 to 3000 m in the Brazil-Falkland Confluence Zone. While the thickness of the NADW decreases toward the south, the NADW types merge. In the Subantarctic Zone between the Subtropical Front and the Subantarctic Front, the NADW properties at the 25°W section are still apparent but with broken and reduced extrema [*Tsuchiya et al.*, 1994].

## 2.6. Antarctic Bottom Water

At the equator the isopycnal  $\sigma_4 = 45.90$  separates the OLNADW from the northward spreading Antarctic Bottom Water (AABW), while near the South Atlantic Current the potential density surface  $\sigma_4 = 45.87$  marks the NADW/AABW boundary [*Stramma and Peterson*, 1990]. The AABW can be separated into two components. The upper part of the AABW originates in the ACC and consists of old deep water masses (Lower Circumpolar Deep Water (LCDW)), while AABW with densities larger than  $\sigma_4 = 46.06$  outflows from the Weddell Sea (Weddell Sea Deep Water) and spreads north-

ward into the Argentine Basin, propagating northward into the Brazil Basin after passing through the Vema Channel, where the water mass has essentially disappeared at 4.5°S [*Siedler et al.*, 1996].

## 3. Lateral Circulation Schemes

Here we propose and discuss the schematic distribution of the mean flow field in the near-surface layer in the upper 100 m (Figure 2), the SACW layer from about 100 to 500 m in the tropics and 600 m in the subtropics (Figure 3), the AAIW layer from about 500 to 1200 m in the tropics and 600 to 1400 m in the subtropics (Figure 4), and the NADW layer at the core at about 2000 m depth (Figure 5). However, the water of the ACC at and south of the Subantarctic Front is Circumpolar Water for all layers presented here. Exact transport rates for the various layer flows are not included, as each study has its own particular definition of layer boundaries. In addition, upwelling and downwelling across the layer interfaces complicate the transport calculations. However, the major regions of water mass formation are indicated. The description of the flow distribution for the tropics north of 20°S is taken from *Stramma and Schott* [1999], so details are not given here. The subtropical distribution is based on the flow patterns at different depths presented by *Reid* [1989, 1994] but modified where more detailed information derived from other more local investigations exist. In the northeastern South Atlantic off Africa there exists the cyclonic Angola Gyre described by *Gordon and Bosley* [1991]. The Angola-Benguela Front oriented northwestward from the African shelf at about 20°S separates the Angola Gyre from the Benguela Current and is well developed in the upper 50 m and detectable in the salinity field to depths of 200 m. In this region, no further southward flow of tropical water is found, different than the layers underneath [*Shannon and Nelson*, 1996].

The subtropical gyre of the South Atlantic is made up of the southward western boundary current, the Brazil Current, which separates from the coast in the confluence zone with the Falkland Current. From there the Brazil Current with admixtures of Falkland Current waters leaves the shelf and flows eastward as the South Atlantic Current. At about 40°W, part of the water recirculates where the Brazil Current Front turns northward [*Smythe-Wright et al.*, 1998] while the major flow continues its eastward path. Some water recirculates west of the Mid-Atlantic Ridge, and a frontal structure in this recirculation region separating two types of Mode Water is also referred to as the Brazil Current Front (Figure 1a) [*Tsuchiya et al.*, 1994]. *Tsuchiya et al.* [1994] also suggest that part of the recirculation extends well into the central South Atlantic. Near South Africa, part of the South Atlantic Current continues to the Indian Ocean while the other part turns north into the Benguela Current and finally into the South Equatorial Current

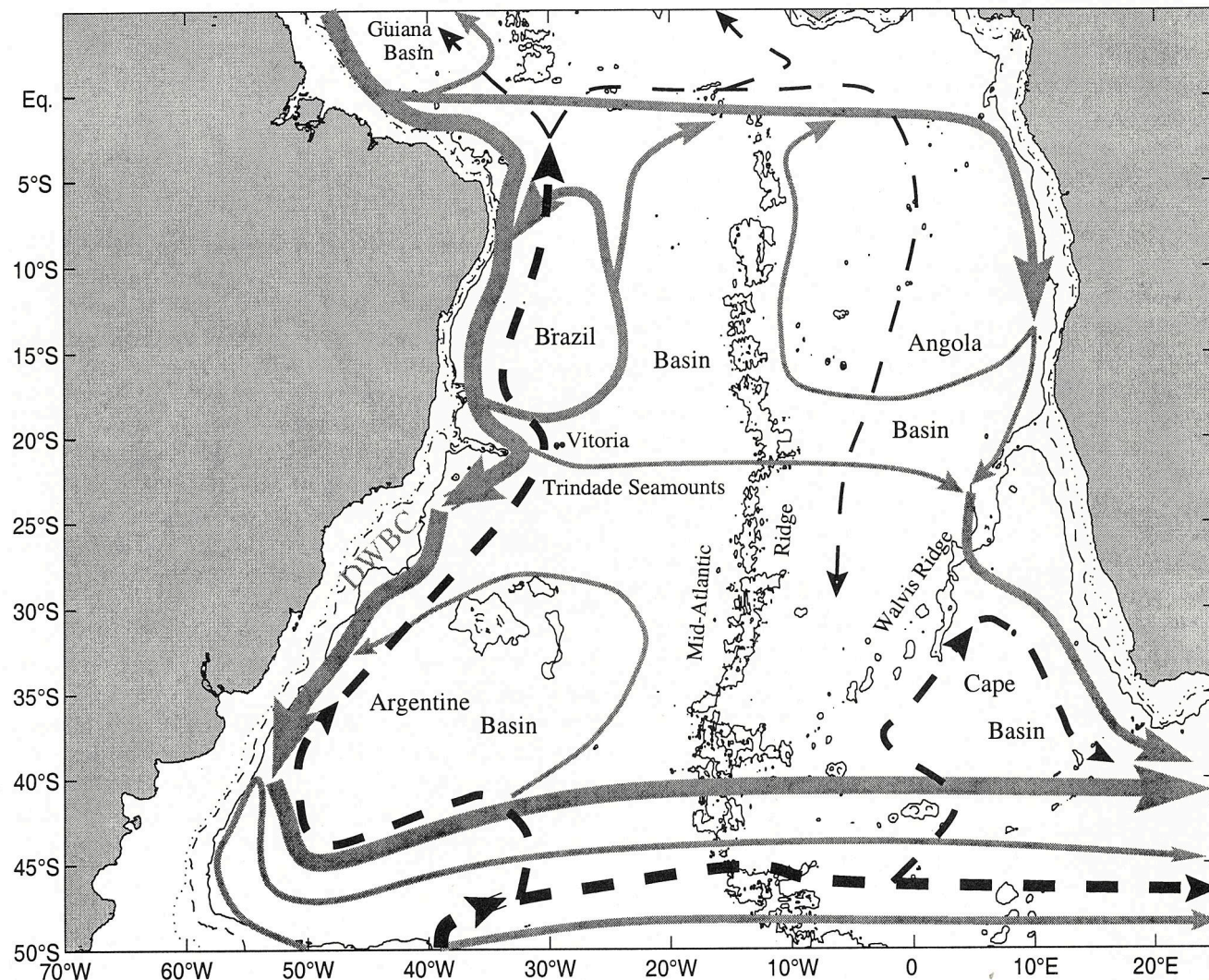


**Figure 5.** Schematic representation of the large scale North Atlantic Deep Water (NADW) water flow near 2000 m depth. The major spreading paths of Antarctic Bottom Water (AABW) are indicated as black lines. Topography is as in Figure 2; in addition, the 3000-m depth contour is shown as a thin solid line.

(SEC). The SEC in the near-surface layer reaches the shelf of Brazil near 16°S and separates into the southward flow of the Brazil Current and at subsurface depth into the northward flow of the North Brazil Undercurrent (NBUC) [Stramma *et al.*, 1995]. The Benguela Current also receives water from the Indian Ocean from a leakage of the Agulhas Current (AC) at its retroflexion south of South Africa [e.g., Lutjeharms, 1996]. The shape of the subtropical gyre depends on the depth layer looked at; the northward extent of the subtropical gyre reduces with increasing depth, while the tropical cyclonic gyre progresses southward. This can be clearly seen in the adjusted steric height figures of Reid [1994], was described by Tsuchiya *et al.* [1994] as wedging of the thermocline in the equatorward side of the subtropical gyre, and reflects a poleward shift with depth of the subtropical gyre. The South Atlantic Current as the southern limb of the subtropical gyre, however, shows no depth-dependent shift.

### 3.1. Near-Surface Layer

The near-surface layer (Figure 2), representing the flow field of the upper 100 m, is the layer with the largest ocean current velocities in most of the regions. At these depths the subtropical gyre shape resembles, for the most part, the shape of the schematic figure of Peterson and Stramma [1991]. The tropical circulation pattern north of 20°S is derived from Stramma and Schott [1999] for all three upper layers; for a detailed description of this region the reader is referred to that article. The different near-equatorial zonal currents shown here were not resolved in the schematic figure of Peterson and Stramma [1991]. Owing to the eastward flow of the South Equatorial Countercurrent (SECC), the South Equatorial Undercurrent (SEUC) and the Equatorial Undercurrent (EUC), the westward flowing SEC is divided into four branches, and they are denoted here as the southern SEC (SSEC), the cent-

ral SEC (CSEC), the equatorial SEC (ESEC), and the northern SEC (NSEC).

Near the equator, off Brazil the SEC overrides the subsurface core of the North Brazil Undercurrent and forms the surface intensified North Brazil Current (NBC), which crosses the equator and is the major source of warm water transfer from the Southern to the Northern Hemisphere. However, this water recirculates in the North Brazil Current Retroflection at about  $5^{\circ}\text{N}$ , part to the EUC, part in northern fall to the North Equatorial Countercurrent (NECC), and part in northern spring toward the Caribbean [Schott *et al.*, 1998], and at deeper levels it contributes also to the North Equatorial Undercurrent (NEUC). In northern spring the NECC is restricted to the central and eastern part of the tropics north of the equator. We show this northern spring situation in Figure 2.

The wind-driven Ekman layer in the upper tens of meters of the ocean might mask the flow structure of the surface water layer at some locations. Most notably, the surface Ekman velocity can mask the surface geostrophic signal of the Angola Gyre [Gordon and Bosley, 1991].

### 3.2. Central Water Layer

For most of the flow field of the South Atlantic Central Water layer (Figure 3) the shape resembles that of the surface layer of Figure 2. However, the northern reaches of the subtropical gyre are shifted more to the south, and the southern band of the South Equatorial Current reaches the Brazilian continent at about  $20^{\circ}\text{S}$  and splits into a weaker part feeding the Brazil Current and a stronger part moving northward as the subsurface core of the North Brazil Undercurrent. In a review of the waters off southwest Africa, Shannon and Nelson [1996] state that thermocline waters and AAIW from the tropical Atlantic are advected poleward off Africa, certainly as far south as  $27^{\circ}\text{S}$  (Figures 3 and 4), which shows that the Angola Gyre is embedded in a large-scale tropical cyclonic gyre (referred to as a "cyclonic subequatorial gyre", [Tsuchiya *et al.*, 1994], with its poleward current band at the northern side of the subtropical gyre. Poole and Tomczak [1999] showed a percentage distribution of the SACW from an optimum multiparameter analysis at 300 and 500 m depth with the western SACW found only within the subtropical gyre, with the northernmost extent at the Brazilian coast at  $20^{\circ}\text{S}$ . They show that eastern SACW enters from the Agulhas region, where the throughflow of eastern SACW occurs between 350 and 600 m and is carried northward mainly with the northern part of the subtropical gyre and spreads within the entire tropical South Atlantic and across the equator, similar to the schematic flow field (Figure 3). According to observations in the southern Benguela Current, Garzoli and Gordon [1996] derived a schematic with a somewhat restricted corridor for Agulhas Current eddy translation, while west of the eddy corridor flows the

South Atlantic source for the Benguela Current and to the east, near the shelf is the Agulhas (Indian Ocean) source. Hence the corridor is breached by South Atlantic and Indian Water as the transient eddy field stirs these water masses.

### 3.3. Intermediate Water Layer

The mean flow field of the AAIW layer is shown in Figure 4. There are two major differences from the flow field above. First, the northern limb of the subtropical gyre shifts farther to the south, reaching the Brazilian continent south of  $20^{\circ}\text{S}$ . According to direct observations of the currents in the AAIW layer by Rafter floats, Pegasus profiles, and current meter data, the northern part of the SSEC reaches the shelf at about  $23^{\circ}\text{S}$  and turns northward while the stronger westward component within the Brazil Current recirculation cell reaches the shelf near  $28^{\circ}\text{S}$  and turns southward [Boebel *et al.*, 1997]. From geostrophic transport estimates of the AAIW, Boebel *et al.* [1997] calculate the separation point between northward and southward flow of AAIW off the Brazilian shelf to be at about  $26^{\circ}\text{S}$ . At the same time the tropical cyclonic gyre extends southward.

Second, the equatorial flow field for the AAIW shows some new features. The flow at the equator changes from eastward above to a westward Equatorial Intermediate Current (EIC) [e.g., Schott *et al.*, 1998], which shows large variability in strength and vertical extent, but nevertheless is a permanent feature. However, owing to the large variability, at times the EIC influences a large part of the SACW layer, leading to eastward currents at the AAIW core level [Stramma and Schott, 1999]. Although permanent, the EIC can lead to reversing currents at the cores of the SACW and AAIW. The EIC is fed by a contribution of two eastward current bands, the Northern Intermediate Countercurrent (NICC) and Southern Intermediate Countercurrent (SICC) at 400 to 1000 m and  $1^{\circ}$ – $3^{\circ}$  north and south of the equator [Schott *et al.*, 1995]. The lowest part of the Angola Gyre, the SEUC, and its return within the ESEC are still visible in water mass distributions but show only weak velocities; hence the currents are included in Figure 4 but presented only by dashed lines.

In the  $30^{\circ}\text{S}$  WOCE section the lowest salinity in the AAIW layer is found in the western basin [Siedler *et al.*, 1996], not in the eastern basin as would be expected if the major transport of AAIW were in the subtropical gyre. Siedler *et al.* [1996] interpret this finding as a northward component of the anticyclonic flow west of the Mid-Atlantic Ridge which supplies less diluted AAIW to the western basin, i.e., a western recirculation as shown in Figure 4. On the basis of CFC distributions, Warner and Weiss [1992] state that more recently ventilated AAIW is apparently transported around the subtropical gyre instead of northward along the western boundary. In addition, as described by Gordon *et al.*

[1992], water from the Indian Ocean enters the AAIW layer south of South Africa, while in the deep water layer, no Indian Ocean to South Atlantic leakage exists.

In the AAIW layer of the tropical cyclonic gyre, high salinity is confirmed in the eastern tropical South Atlantic off Africa along with low oxygen and high nitrate, supporting the notion that vertical mixing as well as biological processes alter the isopycnal properties in that region.

### 3.4. Upper Interocean Exchange

For all three layers of the upper ocean shown in Figures 2-4, there is a flux from the Agulhas into the south-east Atlantic. In the north the South Atlantic loses water to the North Atlantic by cross-equatorial flow, mainly at the western boundary off Brazil. As a result, the South Atlantic receives water from the Indian Ocean and contributes water to the North Atlantic in the near-surface layer, the SACW layer, and the AAIW layer. It is difficult to estimate, from measurements, how strong the water contribution from the South Pacific Ocean to the South Atlantic is through the Falkland Current in the confluence zone with the Brazil Current; nevertheless, exchange, mixing, as well as water mass formation take place in the southwestern South Atlantic. One intriguing feature of all three upper ocean layers is that the separation of the Falkland and the Brazil Currents remains, despite extremely intense eddy activity in the confluence zone.

### 3.5. Upper Circumpolar Deep Water Layer

The UCDW almost disappears near the equator; the vertical extent of this water mass is small in the tropics, and the observed velocities and transports within the UCDW are weak [Fu, 1981]. The exact path of the UCDW is still a controversial issue. The adjusted steric height field of Reid [1989] and the parameter distribution on the WOCE sections [Siedler *et al.*, 1996] point to a circulation within the subtropical gyre. However, a multiparameter analysis suggests that the UCDW progresses northward to about 24°S as a large body of fresh, oxygen-poor, and nutrient-rich water in the western basin and most of it returns southward in the eastern basin [Larqué *et al.*, 1997]. As the cross-equatorial flow of UCDW is weak and the water mass flow path is still not fully known, no circulation scheme is given here for the UCDW.

### 3.6. Deep Water Layer

With increasing depth, NADW spreading paths become more restricted by the topography, and the different water mass components of the NADW will show different spreading paths. Large recirculation cells are proposed for different regions, and flow schematics for different layers indicate exchange of water between the layers [e.g., Friedrichs *et al.*, 1994]. In addition, the NADW layer thickness decreases to the south and the

NADW components merge and mix with the CDW. It is impossible, at present, to construct solid schematics for all four NADW layers, as too few data and some contradictory information exist on the spreading pathways of the different deep layer components. Contradictory results may arise from the different methods used in geostrophic calculations for the deep ocean. In such regions, low velocities can be loaded with large errors and further complicated by large transport variability as observed in the input region for the South Atlantic at the western equatorial boundary [Fischer and Schott, 1997]. While, for example, Durrieu de Madron and Weatherly [1994] showed almost no net transport from the Brazil to the Argentine Basin, the adjusted steric height fields prepared by Reid [1996] show a clear continuation of the DWBC to the Brazil/Falkland Confluence Zone.

According to mooring measurements at the equator at 44°W, the largest inflow of NADW is located in the LSW layer at about 2000 m depth [Fischer and Schott, 1997], and in Figure 5 a schematic flow diagram of the NADW near 2000 m depth (but integrating all NADW components) is presented to show the different behavior of the deep water layer compared to the upper ocean.

When the DWBC reaches the equator, a part of the NADW recirculates in the Guiana Basin [e.g., Friedrichs *et al.*, 1994]; however, the larger part crosses the equator into the South Atlantic. After the DWBC crosses the equator, the NADW separates near a seamount chain at the northeastern tip of Brazil. According to Rhein *et al.* [1995], a large part of the SUNADW continues eastward just south of the equator, while the major part of the LSW follows the DWBC southward. The eastward spreading in the upper part of the NADW was also observed with tracer data in the eastern equatorial Atlantic just south of the equator at 3°50'W [Andrié, 1996]. For the deepest part of the NADW, Friedrichs *et al.* [1994] describe an eastward flow near the equator, and this water enters the eastern basins through the Romanche Fracture Zone.

From the parameter distribution of the large zonal hydrographic WOCE sections presented by Siedler *et al.* [1996], it becomes evident that the major southward transport in the South Atlantic occurs in the DWBC, and a second southward transport band is located near the eastern boundary of the South Atlantic. According to the cumulative transport at 11°S [Speer *et al.*, 1996], the southward transport in the Angola Basin takes place mainly in the upper part of the NADW next to the eastern boundary with recirculation at the eastern flank of the Mid-Atlantic Ridge. Part of the DWBC recirculates in the Brazil Basin [e.g., Durrieu de Madron and Weatherly, 1994; Friedrichs *et al.*, 1994]. A line of seamounts extending offshore near 20°S, known as the Vitoria-Trindade Seamounts, interrupts the DWBC and is the location for eddy formation and apparent flow away from the boundary into the interior [Hogg and Owens, 1999]. From hydrographic measurements it has been speculated that this could feed a narrow

zonal current of the NADW, the "Namib Col Current" [Speer *et al.*, 1995]. At depths of 1300–3000 m near 22°S, this current forms a continuous circulation structure from the western trough to the Namib Col on the Walvis Ridge, indicated by the zonal flow near 22°S in Figure 5. At the Walvis Ridge this water adds to the southward flow from the northern Angola Basin. Evidence suggests that this deep water continues south in the eastern Cape Basin, leaving the South Atlantic near the African continent [Speer *et al.*, 1995]. The float trajectories of Hogg and Owens [1999] suggest that a large portion of the DWBC returns to the western boundary south of the Vitoria-Trindade Seamounts. The results from a multiparameter analysis suggest that there is also a recirculation cell in the Argentine Basin [Larqué *et al.*, 1997].

In the Brazil-Falkland Confluence Zone the DWBC meets the deep-reaching Falkland Current, and near 40°S the NADW leaves the western boundary and mixing of NADW with the CDW creates fine structure in temperature and salinity profiles [Provost *et al.*, 1995]. The measurements along the WOCE section A11 at 45°S in the Argentine Basin and tilted northeastward east of the Mid-Atlantic Ridge to 30°S, near the African continent shed light on the eastward flow of NADW. Just east of the Falkland Current, 15 Sv of deep water cross the 45°S section, but all returns northward west of 38°W. In the tilted northeast part of the A11 section in the Cape Basin the major NADW component flows eastward south of 40°S with an additional southward flow near the African continent [Saunders and King, 1995]. The water mass distribution shows that the NADW southward extent is terminated near 45°S [Peterson and Whitworth, 1989], where the northern band of the Antarctic Circumpolar Current connected to the Subantarctic Front (SAF) (see also Figure 1a) penetrates to great depth. Hence the NADW is flowing eastward at the location of the South Atlantic Current near 40°S and in the Subantarctic Zone north of the SAF, in good agreement with the NADW distribution near 25°W observed by Tsuchiya *et al.* [1994]. South of the SAF, Circumpolar Deep Water is located at deep water depths. At the location of the Falkland Current and its extension as the northern band of the ACC and to the south, Circumpolar Deep Water is flowing eastward. However, detached masses of NADW were observed within the CDW at the western boundary as well as within the ACC south of the SAF in the south central Argentine Basin [Peterson and Whitworth, 1989]. This shows that in the Brazil-Falkland Confluence Zone some admixture of NADW into the CDW layer takes place.

### 3.7. Antarctic Bottom Water Layer

The spreading of the AABW is strongly influenced by the bottom topography. As for the UCDW component, the cross-equatorial flow of AABW is weak [e.g., Rhein *et al.*, 1998]. The major spreading paths of AABW are included as dashed lines in Figure 5, but basin-scale de-

tails as derived, for example, from a few sections in the Brazil Basin by Durrieu de Madron and Weatherly [1994] are not included. Owing to the topography, the AABW enters the Argentine Basin at the southeastern side and flows to the western boundary in the deep Argentine Basin. It is the LCDW component of the AABW that spreads northward mainly in the western basins of the South Atlantic and crosses the equator to the Northern Hemisphere. It also spreads eastward at the equator through the Romanche Fracture Zone to fill the Angola Basin from the north. AABW eventually flows into the eastern basin of the North Atlantic. Owing to the barrier of the Walvis Ridge, the Cape Basin receives AABW from the south, and near the African continent this water returns south toward the Agulhas region [e.g., Saunders and King, 1995].

## 4. Model Simulations in the South Atlantic

Modeling strategies for the South Atlantic Ocean have been discussed by Barnier *et al.* [1996]. The South Atlantic Ocean is widely open to the Indian Ocean and the North Atlantic Ocean and has a large inflow from the Pacific through the more narrow Drake Passage. Important property fluxes take place across these three open boundaries. Hence strategies of modeling the ocean circulation in this area require a consideration of interocean exchange at these three sections. Approaches to study the South Atlantic are either to model the world ocean and study the South Atlantic as a subdomain [e.g., England and Garçon, 1994] or to limit the model domain to the South Atlantic basin and then deal with the complicated problem of open boundaries [e.g., Matano and Philander, 1993; Barnier *et al.*, 1996; Marchesiello *et al.*, 1998]. While the first approach can exhibit large differences between the various hydrographic and model estimates of fluxes at the limits of the South Atlantic (even at eddy-resolving resolutions), the second approach largely depends upon the fluxes prescribed at the open boundaries [Barnier *et al.*, 1996]. Regional South Atlantic Ocean models can therefore be tuned somewhat by adjusting the prescribed open boundary conditions.

In this section we directly compare two global ocean GCMs with the observations of the mean circulation in the South Atlantic described above. While the two models are both run over a global domain and each uses a Z-level vertical coordinate system and similar numerics, they differ substantially in horizontal resolution; one is coarse (just under 2° resolution) and does not resolve mesoscale eddies or detailed bathymetry, the other is high resolution and eddy permitting. Intercomparing two global ocean models in this manner helps determine what circulation patterns in the South Atlantic are resolved at different model resolutions. Vector plots from a regional South Atlantic model were not included explicitly in our analyses as (1) most are limited to the

north at 15°S and we are also interested in the equatorial current structure, (2) the regional model solution is determined in part by the prescribed open boundary conditions, and (3) the resolution of regional South Atlantic models is generally no higher than that adopted in high-resolution global studies. Some reference will be made, nevertheless, to the simulated circulation in the  $\sigma$  coordinate regional South Atlantic model of *Marchesinello et al.* [1998].

#### 4.1. Model Descriptions

The resolution and geometry of the coarse model are typical of state-of-the-art coupled ocean-atmosphere models used to study climate variability and anthropogenic climate change. Its configuration and mixing coefficients are described by *England and Garçon* [1994]. The ocean model is the Geophysical Fluid Dynamics Laboratory (GFDL) Modular Ocean Model (MOM) and is based upon the primitive equations for the ocean circulation [*Bryan*, 1969; *Cox*, 1984; *Pacanowski et al.*, 1991]. The resolution is coarse (1.8° in longitude and 1.6° in latitude), so the eddy field is not resolved explicitly. There are 33 unequally spaced vertical levels with bottom topography and global continental outlines as realistic as possible for the given grid box resolution.

The coarse model is driven by *Hellerman and Rosenstein* [1983] winds. The model temperature and salinity are relaxed to the climatological annual mean fields of *Levitus* [1982] at the surface and below 700 m. The coarse model run is therefore in diagnostic mode below 700 m, whereas it freely equilibrates above this depth. The restoring terms are weak below 700 m and act mainly to suppress vertical motions and convection rather than influence the lateral circulation schemes shown here. The subsurface T-S restoring ensures rather rapid baroclinic adjustment and shorter model equilibration times and limits deep water mass drift. From this model the velocity distribution at 90 m depth (Figure 6) was chosen to represent the upper ocean currents, that at 430 m (Figure 7) represents the SACW layer and that at 900 m (Figure 8) represents the AAIW layer. The deep layer circulation field is represented by the ocean currents at about 2250 m depth (Figure 9).

The fine resolution model included in our analyses is the Parallel Ocean Climate Model (POCM) with nominal lateral resolution of 1/4° [*Stammer et al.*, 1996; *Tokmakian*, 1996] based on the model formulation of *Semtner and Chervin* [1992]. The model domain is nearly global, running from 75°S to 65°N. The actual grid is a Mercator grid of size 0.4° in longitude, yielding square grids everywhere between the equator and 75° latitude [*Stammer et al.*, 1996]. The resulting average grid size is 1/4° in latitude. Model bathymetry was derived by a grid cell average of actual ocean depths over a resolution of 1/12°. Unlike our coarse model, the fine resolution model includes a free surface [after *Kill-*

*worth et al.*, 1991] that treats the sea level pressure as a prognostic variable.

The POCM experiment was integrated for the period 1987 through to June 1998 using European Centre Medium-Range Weather forecasts (ECMWF) derived daily wind stress fields, climatological monthly mean ECMWF sea surface heat fluxes (produced by *Barnier et al.* [1995]), and some additional  $T$ ,  $S$  surface restoring terms. The surface restoring of  $T$  and  $S$  adopts the *Levitus et al.* [1994] monthly climatology with a 30-day relaxation timescale (similar to *England and Garçon* [1994] (hereafter referred to as EG94)). Subsurface to 2000-m depth T-S are also restored toward *Levitus* [1982] along artificial model boundaries north of 58°N and south of 68°S to approximate the exchange of water properties with those regions not included in the model domain. The timescale for relaxation used in these boundary domains is 120 days. Elsewhere, the model T-S freely equilibrates. The POCM is therefore prognostic, although it should be noted that with limited integration times the deep water masses are changed little from their initial conditions (i.e., the *Levitus* [1982] climatology). Thus both models have a realistic deep water mass structure owing to interior T-S restoring terms (EG94) and short model integration times (POCM). Further model details are given by *Semtner and Chervin* [1992], *Stammer et al.* [1996], and *Tokmakian* [1996].

To intercompare the high-resolution POCM with the model of *England and Garçon* [1994] and the observations described above, we include plots of simulated POCM ocean currents at 87.5, 435, 847.5, and 2475 m in Figures 6-9, respectively. It may be noted that the plotted POCM currents are drawn over a coarser grid than that actually simulated; in particular, vectors are drawn at every third grid box in latitude and longitude (with no spatial averaging).

#### 4.2. Model-Model Comparison

In many respects the coarse resolution and fine resolution models exhibit similar circulation patterns in the South Atlantic. For example, they both simulate a strong and shallow EUC, a gradual reduction in northward extent of the subtropical gyre with depth, and a direct Indian to Atlantic transport of upper water via the Agulhas Current. The differences between the models often relate to narrower and faster ocean currents in the fine resolution simulation, such as an explicitly resolved South Atlantic Current north of the ACC. In addition, the eddy-permitting model exhibits rich mesoscale structure in the ACC and a more complex equatorial current system in the upper 100 m. However, many aspects of the observed circulation are not captured by either model, and in some instances the coarse model happens to be more realistic (e.g., in simulating the Angola Gyre). Details of the model-observation compar-

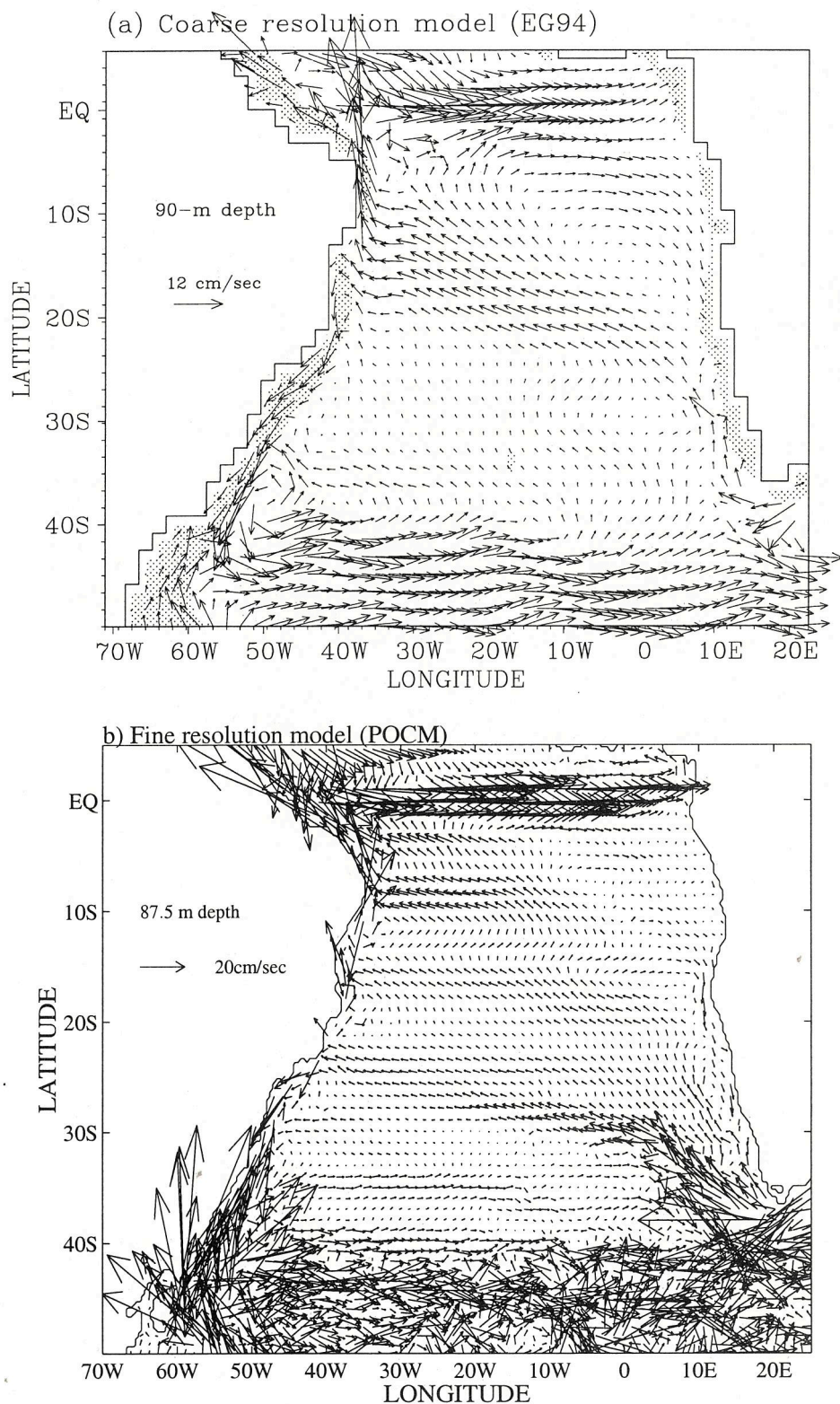


**Figure 6.** Horizontal ocean currents simulated in the South Atlantic Ocean near 90 m in (a) our coarse resolution model and (b) the eddy-permitting Parallel Ocean Circulation Model (POCM) simulation (courtesy of R. Tokmakian, Naval Postgraduate School). In Figure 6a, areas with model topography of less than 3000 m are stippled. In the Figure 6b, only every third ocean model vector is plotted. Note that vector scaling differs between the coarse and fine resolution diagrams.

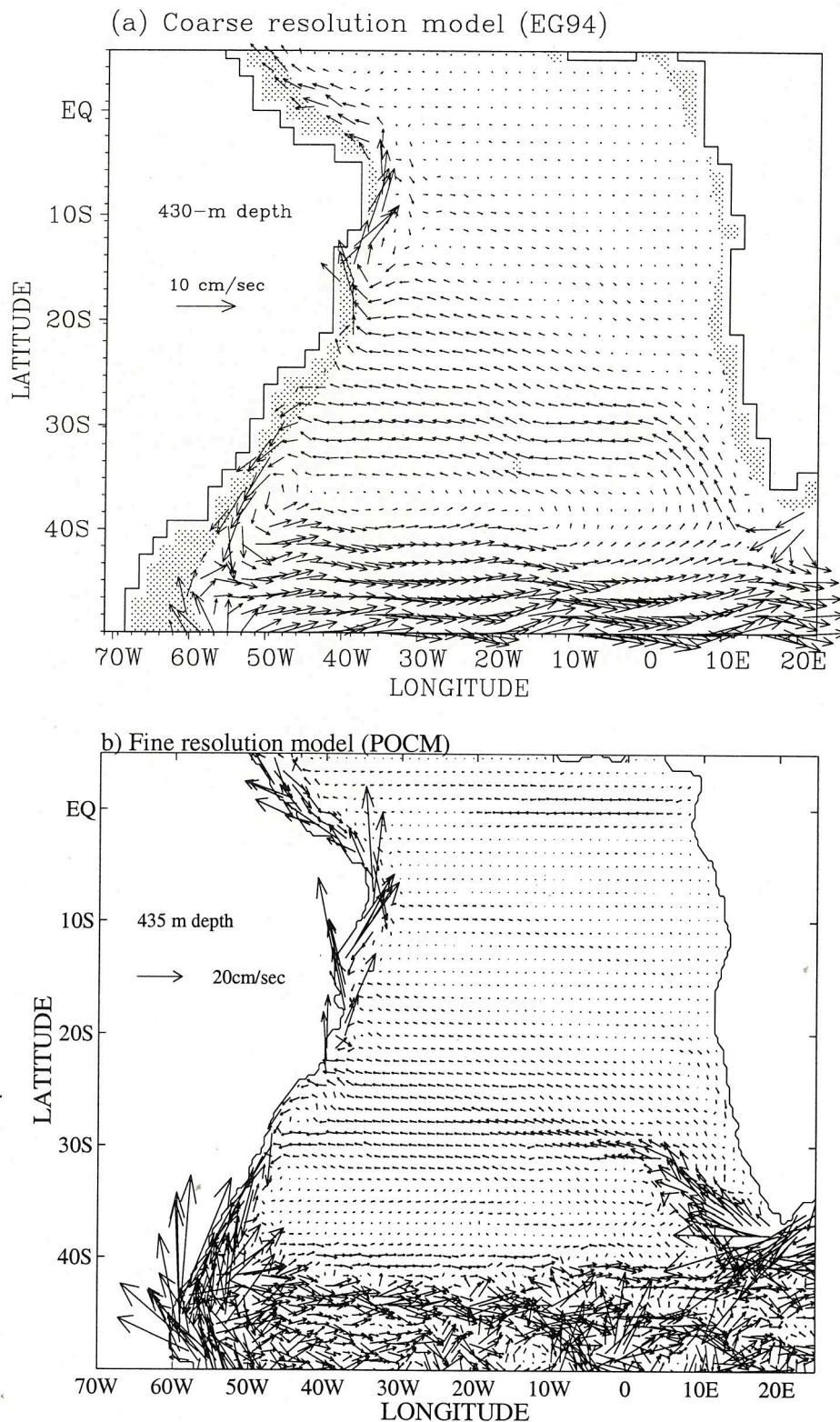


Figure 7. Same as Figure 6, but for 430-m depth.

ison for each depth layer considered in section 3 will now be discussed.

#### 4.3. Model-Observation Comparisons

**4.3.1. Near-surface layer.** Near 90 m depth (Figure 6), the coarse model shows a South Equatorial

Current that widens near the South American continent and reaches the coastal region at  $10^{\circ}$  to  $18^{\circ}\text{S}$ . In contrast, the POCM model simulates a much narrower SEC fed by the northern limb of the Benguela Current arriving at the South American coast near  $15^{\circ}\text{S}$  (as observed). In addition, a stronger westward flowing cur-

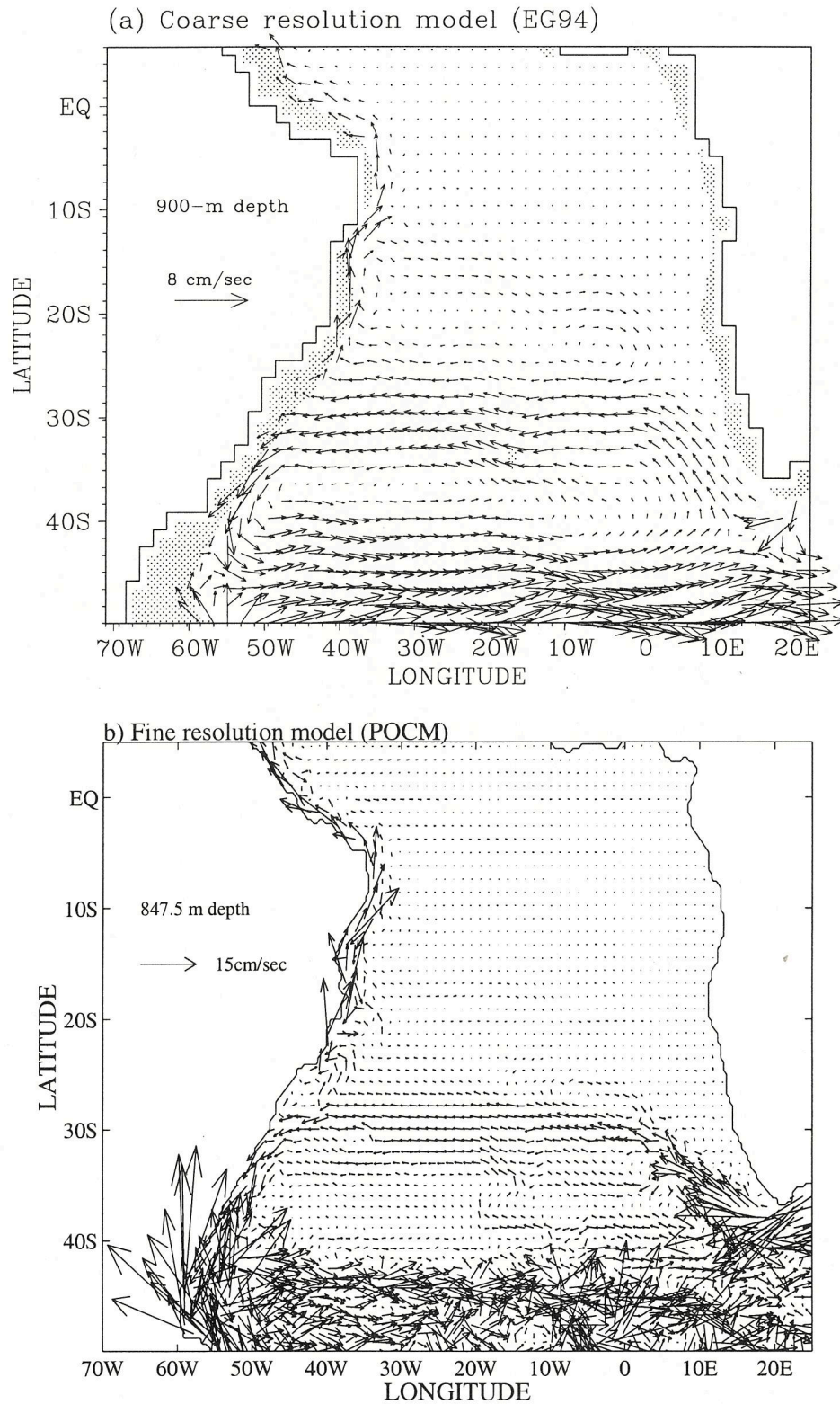


**Figure 8.** Same as Figure 6, but at 850- to 900-m depth.

rent is simulated near 25°–30°S in the eddy-permitting model, with water south of Africa advected toward the center of the subtropical gyre. This feature is absent in the coarse model. In observations, Agulhas rings have been noted to cross the Walvis Ridge farther south than

the mean surface field of Figure 2, seeking out deeper topography and moving across the South Atlantic near the center of the subtropical gyre [see *Lutjeharms*, 1996; Figure 15]. The POCM experiment, with marginally resolved eddies at this latitude, reproduces this preferred

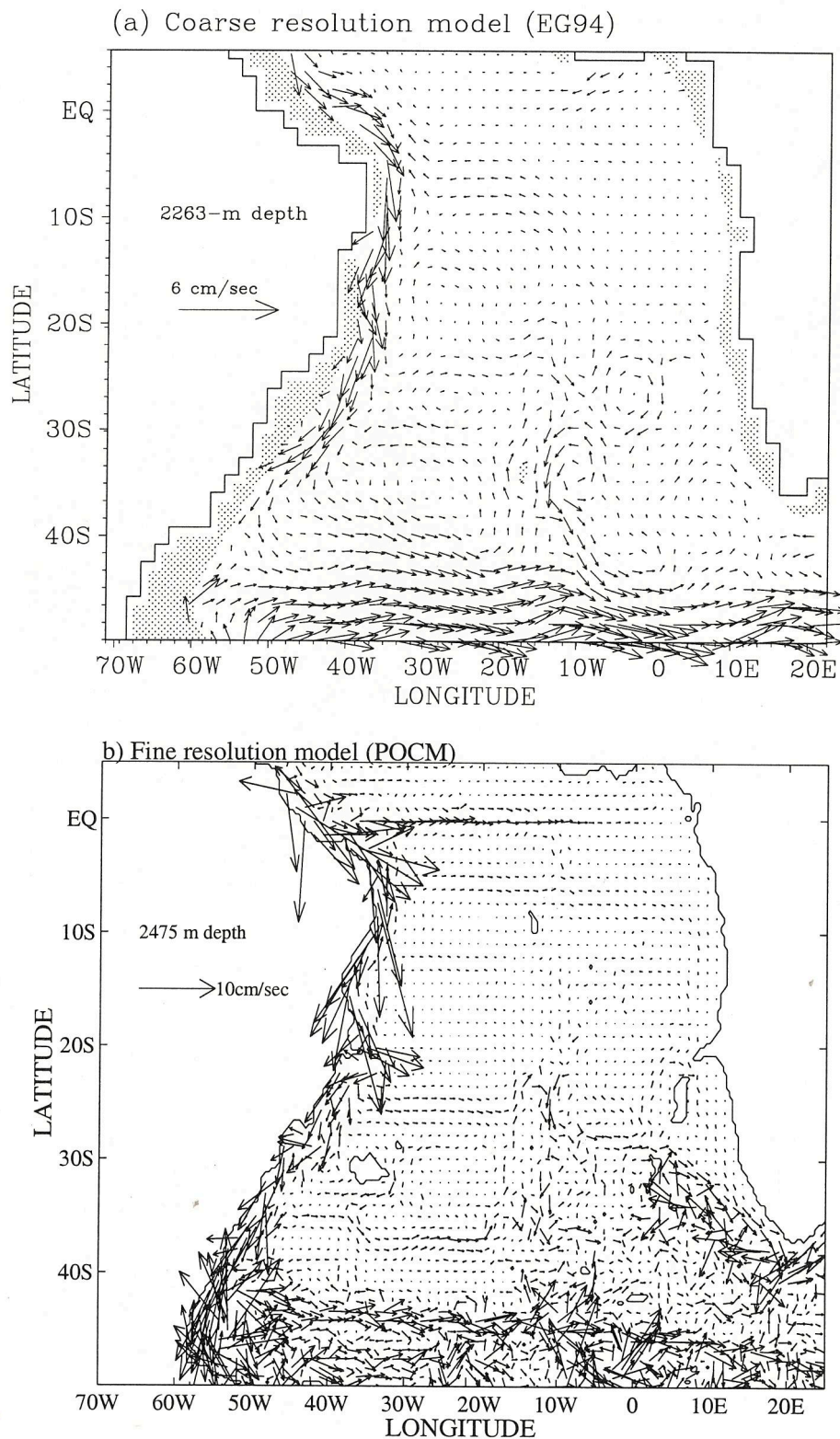


**Figure 9.** Same as Figure 6, but for depth levels near 2200-2500 m.

Agulhas ring path to the west, although it is too regular and slightly too far to the north (R. Tokmakian, personal communication, 1999).

While the fine resolution model captures some of the meridional structure in the zonal currents north of 15°S, the coarse model simulates only a broad EUC. Both

models produce a cross-equatorial flow off Brazil and a southward recirculation loop feeding the Equatorial Undercurrent. However in both models, particularly the coarse version, the EUC is somewhat too wide. The coarse model captures the Angola Gyre in the eastern tropical South Atlantic, although it is essentially bound

to the north by the EUC and to the south by the SEC. The fine resolution model does not simulate an Angola Gyre with the same spatial extent as observed. In particular, the POCM sees the gyre centered farther to the south, separated from the equatorial currents, with only a limited poleward flowing eastern boundary current near  $15^{\circ}$ – $20^{\circ}$ S.

The Brazil-Falkland Confluence is close to the location described from hydrographic and satellite observations in both models (and in the model of *Marchesiello et al.* [1998]). However, the coarse model does not separate the South Atlantic Current from the ACC, whereas the POCM does. In addition, the coarse model flow structure is dominated by topographic steering of the ACC in the Southern Ocean. This is also true of the fine resolution model, although significant internal eddy variability also characterizes the region. In both model cases the Benguela Current originates off South Africa, fed by a mixture of saline water of the Indian Ocean and water from the subtropical South Atlantic. However, in the POCM run some of this Agulhas leakage occurs via mesoscale eddies, as observed.

**4.3.2. Agulhas leakage.** The water mass transfer from the Indian to the South Atlantic is difficult to measure, as it is caused by highly time variable processes. Estimates from earlier observations reviewed by *Peterson and Stramma* [1991] were in the range of 3 to 15 Sv, and recent results listed by *Lutjeharms* [1996] seem to converge to values in the middle of the range of the earlier observations, i.e., around 8 Sv or so. Total Agulhas leakage transport is 8.7 Sv in the coarse model; all of this water is advected northward into the Benguela Current [*England and Garçon*, 1994]. The Agulhas leakage transport is substantially higher in the POCM run, with over 90 Sv advected westward across  $20^{\circ}$ E and north of  $39^{\circ}$ S (R. Tokmakian, personal communication, 1999). However, a substantial component of this transport recirculates into the ACC, with only 24.2 Sv flowing northward across  $30^{\circ}$ S within the Benguela Current. Even an Agulhas leakage of 24.2 Sv is somewhat larger than Indian to South Atlantic water transfer rates estimated from observations. Analyses of interocean exchange of heat and freshwater are being carried out in this region to determine the relative success of models at capturing thermohaline transports in the Agulhas leakage.

**4.3.3. Central Water layer.** The 430-m distribution (Figure 7) shows the southward shift of the subtropical gyre in both models, reaching the South American continent in a wide region between  $15^{\circ}$  and  $32^{\circ}$ S. In the fine resolution model the NBUC is narrower and faster than its coarse model counterpart, traveling at speeds of up to  $50 \text{ cm s}^{-1}$ . At this depth, neither model reproduces the weak Angola Gyre or the zonal equatorial current structure. In the POCM run the westward flowing Equatorial Intermediate Current (which is not strongly confined to the water mass boundaries [*Stramma and Schott*, 1999]) is seen on the eastern side

along the equator at 435 m depth. In fact, the EIC does not appear near 900 m depth in either model (Figure 8), and no signature of the eastward flowing EUC is seen in the model Central Water near 430 m. This is not a problem in the POCM, as it sees a shallow EIC which is not in disagreement with observations, recalling the EIC spatial variability noted in section 3. However, in the coarse model, virtually no equatorial ocean flow is seen along the equator in the Central Water layers.

Both models show the cross-equatorial flow from the Southern to the Northern Hemisphere in the western equatorial Atlantic off Brazil. The fine resolution model further captures the southward flowing recirculation fed by the North Brazil Current, although it flows south to  $10^{\circ}$ S, feeding a weak SEUC instead of separating from the coast at the equator. Both models capture the contribution of Central Water from the Indian Ocean via the Agulhas Current into the South Atlantic. However, the equatorial currents are weak or erroneous near 430 m depth in both coarse and fine models, apart from the shallow EIC in the POCM simulation. Capturing the complex meridional structure of the equatorial current system in the SACW layer certainly requires higher horizontal resolution than we use in the coarse model and perhaps higher vertical resolution or a more realistic parameterization of vertical momentum transfer in the eddy-permitting model.

**4.3.4. Intermediate Water layer.** The 850-to-900-m distribution (Figure 8) representing the AAIW layer shows the subtropical gyre farther to the south in both fine and coarse models. The splitting of the flow of AAIW south of  $25^{\circ}$ S is in agreement with WOCE float observations [e.g., *Boebel et al.*, 1997]. The westward flow of intermediate water bifurcates at the coast into the northward flowing NBUC and the southward flowing Brazil Current, as observed. In the tropics the cross-equatorial flow is present; however, the zonal tropical currents are not resolved at all in the coarse model (most likely a problem of low model resolution). The higher-resolution POCM only simulates weak equatorial flow at this depth and, in fact, has an equatorial current flowing in the opposite direction to the EIC. The EIC is known for large variability in vertical extent, and the fine resolution model appears to be simulating it at 300–500 m depth, leaving very weak eastward flows at the deeper 847-m surface shown here. Apart from this weak equatorial current just off Brazil, there is virtually no zonal flow in either model at the tropical latitudes. Further model studies of the equatorial Atlantic circulation are required to determine why models behave so poorly in the context of capturing the tropical circulation system in the upper South Atlantic.

Farther to the south, both models capture the ACC, rich in mesoscale structure in the POCM. Both models also capture the water contribution from the Indian Ocean to the South Atlantic via the Agulhas Current at intermediate layers. A weak contribution of northward flowing intermediate water on the western flank

of the Mid-Atlantic Ridge can be seen in the POCM (near 20°W). In contrast, this flow is missing in the coarse resolution model. Like the POCM, the  $\sigma$  coordinate model of *Marchesiello et al.* [1998] captures a northward flow of AAIW near 20°W and proposes a circulation very consistent with the above scheme for AAIW (Figure 4). Details of model topography at the Mid-Atlantic Ridge probably determine the nature of intermediate water flow in this region.

**4.3.5. Deep Water layer.** The flow simulations near 2000–2500 m depth are used to analyze the deep water circulation schemes in the coarse and fine resolution models. Both models put most of their NADW outflow in the Deep Western Boundary Current off South America. The DWBC separates from the coast in a broad region near 35°–42°S in the coarse model, whereas in the fine model a more distinct confluence with the northward flowing Falkland Current is simulated near 40°S. Only the fine resolution POCM captures the equatorial excursion of NADW eastward, resulting in a weak poleward flow of NADW at the eastern boundary of the Angola Basin.

Both models capture the eastward circulation of NADW from the DWBC at 20°S, i.e., the Namib Col Current of *Speer et al.* [1995]. The coarse model sees much of this flow turn southward at the Mid-Atlantic Ridge with only a weak outflow in the eastern Cape Basin. The fine model, on the other hand, simulates substantial NADW outflow along the eastern boundary complicated by small-scale recirculations in the region. The model of *Marchesiello et al.* [1998] also captures a Namib Col Current, although it is very broad and some of it recirculates northward along the eastern boundary. Both model runs considered herein also capture a recirculation cell in the Argentine Basin (as advocated by *Larqué et al.* [1997]). This is quite a broad flow in the coarse model; in contrast, the POCM simulates a distinct boundary current separation near 35°S flowing eastward and recirculating anticlockwise within the Argentine Basin. Overall, both global coarse and fine models do a reasonable job at capturing the deep water circulation patterns in the South Atlantic Ocean.

**4.3.6. Antarctic Bottom Water layer.** Bottom water flow patterns in ocean circulation models depend primarily on the production rate of AABW and the choice of model bathymetry. So long as reasonable amounts of AABW are formed, the model circulation pathways will be quite realistic if a reasonable distribution of bottom topography is incorporated into the model. In both models considered here, AABW formation rates are quite weak. This is probably because of the interior restoring terms in the coarse model and the short integration times in the POCM run. Short integration times mean that the fine resolution model has interior T-S still quite close to its initial conditions (i.e., the *Levitus* [1982] climatology), rendering weak interior overturning rates as described by *Toggweiler et al.* [1989]. In addition, neither model incorporates sea

ice formation processes explicitly, relying on climatological salinity forcing to approximate wintertime brine rejection as sea ice is formed. This is known to limit AABW formation rates in ocean models because of a lack of wintertime observations of Antarctic salinities under sea ice [*England, 1992*].

In spite of weak AABW formation rates in both models, there is general agreement between the model runs and observed AABW flow patterns in the deep basins. For example, bottom waters enter the Argentine Basin flowing northward along the western boundary. Only a very weak cross-equatorial flow is simulated, however, as AABW formation rates are low (2–3 Sv total). Bottom water inflow and recirculation in the Cape Basin are also captured by both models, although they are very weak. In comparison, *Marchesiello et al.* [1998] simulate AABW northward flow in the central Argentine Basin (see their Figure 11), although they capture more northward flow east of the Vitoria-Trindade Seamounts. These simulated circulation patterns are highly dependent on model bathymetry details and AABW overturning strength.

Coarse models that capture stronger AABW formation rates appear to reproduce the flow schematic of Figure 5 rather well. For example, northward flowing signatures of young CFC-laden bottom waters are simulated by *England et al.* [1994] and *England* [1995], with a western boundary flow continuing from the Argentine and Brazil Basins into the North Atlantic and some equatorial recirculation of AABW eastward into the Angola Basin. The bottom water in the Angola Basin then flows southward. A Cape Basin circulation of AABW is also captured by the coarse model of *England et al.* [1994] and *England* [1995]. It would appear, then, that within the limits of model bathymetry matching the observed South Atlantic, bottom water flow patterns are quite well resolved if a sufficiently high rate of AABW is produced in the Weddell Sea.

## 5. Conclusions

Schematic circulation diagrams based on observational evidence have been presented for the near-surface layer, the South Atlantic Central Water, the Antarctic Intermediate Water, and the North Atlantic Deep Water of the South Atlantic. These reveal differences in the mean circulation of the different water masses and present a more complete view of the vertical structure of the mean circulation than available in previous studies. However, there are large regions where the flow field was not resolved by detailed observations. While in the upper ocean the subtropical South Atlantic is governed by the subtropical gyre with a southward shift of the northern part of the gyre, the tropical circulation shows several depth-dependent zonal current bands. In the NADW layer the southward transport takes place mainly in the Deep Western Boundary Current to the Brazil/Falkland Confluence Zone, from where the NADW is transported

eastward. Although much contradictory information on the NADW water spreading in the South Atlantic exists, the recent WOCE measurements seem to prove that southward transport also takes place at the eastern boundary, in good agreement with a multiparameter analysis of water masses in the South Atlantic [Larqué *et al.*, 1997].

A coarse resolution global ocean GCM and a global eddy-permitting model were analyzed to assess the ability of ocean models to capture the observed circulation in the South Atlantic. The models both resolved the southward shift of the subtropical gyre. However, neither model could reproduce the zonal current system of the tropical South Atlantic, certainly owing to insufficient meridional resolution in the coarse model and possibly to insufficient vertical resolution in the fine model. In addition, surface forcing fields might lack the observed meridional structure in wind stress gradients in the tropical oceans in the POCM experiment. This is a subject of ongoing research in the POCM simulation.

All observations show that the subtropical gyre and the southward shift with depth of its northern branch are robust features of the South Atlantic circulation. These are reproduced in our coarse resolution GCM and the POCM. Other robust features of the coarse and fine models are the interhemispheric exchange from the South to the North Atlantic in the western equatorial region, the water leakage from the Indian Ocean to the South Atlantic via the Agulhas Current, and the confluence of the Brazil and Falkland Currents. The fine resolution model captures narrower and faster ocean currents than the coarse model, such as an explicitly resolved South Atlantic Current north of the ACC. In addition, the eddy-permitting model exhibits rich meso-scale structure in the ACC and a more complex equatorial current system. Still unclear from observations is how the Falkland and Brazil Currents interact and exchange water, hence how strong the input from the South Pacific to the South Atlantic is. From model results, estimates of this exchange can be derived; for example, in the same model as we have used, England and Garçon [1994] find a 6.5 Sv contribution from the Drake Passage to the South Atlantic northward transport toward the North Atlantic.

The schematic flow fields derived from observations (Figures 2-5) are supposed to present the mean circulation within a water mass layer; however, the current bands are not closely connected to the water mass boundaries (especially in the tropics). In addition, upwelling and downwelling take place between the layers. This leads to an exchange of water between the layers. One such calculation was performed by Speer *et al.* [1996], who derived a net geostrophic volume northward transport at 11°S of 34.8 Sv for the upper ocean. In a comparison with the results from other sections at 14°N and 45°-30°S, they compute a southward Ekman transport at 11°S of 12 Sv and to the north at 14°N of 14 Sv. Together with the derived ocean layer transports, they

estimate a flow of 26 Sv into the Ekman layer between 11°S and 14°N and of 17 Sv from the Ekman layer into the geostrophic circulation between 11°S and 45°-30°S. Although proven to be important, exactly where and to what extent upwelling and downwelling take place is far from being resolved; hence such processes are not indicated in the flow field schematics. Despite this lack of information on water mass exchange across layer interfaces, the schematic flow fields presented can be used as a comparison of the horizontal flow field of detailed surveys of special areas, in qualitative ocean model assessments, and for the investigation of deviations from the mean horizontal circulation.

**Acknowledgments.** Financial support was received through the German WOCE program by Bundesministerium für Bildung, Wissenschaft, Forschung und Technologie (BM-BF) under grants 03F0157A and 03F0176A and from the Australian Research Council. R. Tokmakian and A. Semtner are gratefully acknowledged for providing ocean model output and graphics from the Parallel Ocean Climate Model, as well as giving feedback on a draft version of this paper. Arnold Gordon and three anonymous reviewers made valuable comments on the original version of this manuscript.

## References

- Andrié, C., Chlorofluoromethanes in the Deep Equatorial Atlantic revisited, in *The South Atlantic: Present and Past Circulation*, edited by G. Wefer *et al.*, pp. 273-288, Springer-Verlag, New York, 1996.
- Barnier, B., L. Siefried, and P. Marchesiello, Thermal forcing for a global ocean circulation model using a 3-year climatology of ECMWF analyses, *J. Mar. Syst.*, **6**, 363-380, 1995.
- Barnier, B., P. Marchesiello, and A.P. de Miranda, Modeling the ocean circulation in the South Atlantic: A strategy for dealing with open boundaries, in *The South Atlantic: Present and Past Circulation*, edited by G. Wefer *et al.*, pp. 289-304, Springer-Verlag, New York, 1996.
- Boebel, O., C. Schmid, and W. Zenk, Flow and recirculation of Antarctic Intermediate Water across the Rio Grande Rise, *J. Geophys. Res.*, **102**, 20,967-20,986, 1997.
- Bryan, K., A numerical method for the study of the circulation of the World Ocean, *J. Comput. Phys.*, **3**, 347-376, 1969.
- Cox, M.D., A primitive equation, three-dimensional model of the ocean, GFDL Ocean Group Tech. Rep. 1, 143 pp. Geophys. Fluid Dyn. Lab., Princeton, N. J., 1984.
- Durrieu de Madron, X., and G. Weatherly, Circulation, transport and bottom boundary layers of the deep currents in the Brazil Basin, *J. Mar. Res.*, **52**, 583-638, 1994.
- England, M.H., On the formation of Antarctic Intermediate and Bottom Water in ocean general circulation models, *J. Phys. Oceanogr.*, **22**, 918-926, 1992.
- England, M.H., The age of water and ventilation time-scales in a global ocean model, *J. Phys. Oceanogr.*, **25**, 2756-2777, 1995.
- England, M.H., and V.C. Garçon, South Atlantic circulation in a general circulation model, *Ann. Geophys.*, **12**, 812-825, 1994.
- England, M.H., V.C. Garçon, and J-F. Minster, Chlorofluorocarbon uptake in a World Ocean model, 1, Sensitivity to the surface gas forcing, *J. Geophys. Res.*, **99**, 25,215-25,233, 1994.

- Fischer, J., and F. Schott, Seasonal transport variability of the Deep Western Boundary Current in the equatorial Atlantic, *J. Geophys. Res.*, 102, 27,751-27,769, 1997.
- Friedrichs, M.A.M., M.S. McCartney, and M.M. Hall, Hemispheric asymmetry of deep water transport modes in the Atlantic, *J. Geophys. Res.*, 99, 25,165-25,179, 1994.
- Fu, L.-L., The general circulation and meridional heat transport of the subtropical South Atlantic determined by inverse methods, *J. Phys. Oceanogr.*, 11, 1171-1193, 1981.
- Fu, L.-L., The circulation and its variability of the South Atlantic Ocean: First results from the TOPEX/POSEIDON mission, in *The South Atlantic: Present and Past Circulation*, edited by G. Wefer et al., pp. 63-82, Springer-Verlag, New York, 1996.
- Garzoli, S.L., and A.L. Gordon, Origins and variability of the Benguela Current, *J. Geophys. Res.*, 101, 897-906, 1996.
- Gordon, A.L., South Atlantic thermocline ventilation, *Deep Sea Res., Part A*, 28, 1239-1264, 1981.
- Gordon, A.L., and K.T. Bosley, Cyclonic gyre in the tropical South Atlantic, *Deep Sea Res., Part A*, 38, suppl., S323-S343, 1991.
- Gordon, A.L., R.F. Weiss, W.M. Smethie Jr., and M.J. Warner, Thermocline and intermediate water communication between the South Atlantic and Indian Oceans, *J. Geophys. Res.*, 97, 7223-7240, 1992.
- Hellerman, S., and M. Rosenstein, Normal monthly wind stress over the world ocean with error estimate, *J. Phys. Oceanogr.*, 13, 1093-1104, 1983.
- Hogg, N.G., and W.B. Owens, Direct measurements of the deep circulation within the Brazil Basin, *Deep Sea Res., Part II*, 46, 305-333, 1999.
- Killworth, P.D., D. Stainforth, D.J. Webb, and S.M. Paterson, The development of a free-surface Bryan-Cox-Semtner ocean model, *J. Phys. Oceanogr.*, 21, 1333-1348, 1991.
- Larqué, L., K. Maamaatuaiahutapu, and V. Garçon, On the intermediate and deep water flows in the South Atlantic Ocean, *J. Geophys. Res.*, 102, 12,425-12,440, 1997.
- Levitus, S., Climatological atlas of the world ocean, *NOAA Prof. Pap.* 13, 173 pp., U.S. Govt. Print. Off., Washington, D.C., 1982.
- Levitus, S., T.P. Boyer, and J. Antonov, World Ocean Atlas 1994, vols. 1-4, *NESDIS Atlas 1-4*, 162 pp., Nat. Oceanogr. Data Cent., NOAA, Silver Spring, Md., 1994.
- Lutjeharms, J.R.E., The exchange of water between the South Indian and South Atlantic Oceans, in *The South Atlantic: Present and Past Circulation*, edited by G. Wefer et al., pp. 125-162, Springer-Verlag, New York, 1996.
- Maamaatuaiahutapu, K., C. Provost, C. Andrieu, and X. Vigan, Origin and ages of mode waters in the Brazil-Malvinas Confluence region during austral winter 1994, *J. Geophys. Res.*, this issue.
- Marchesiello, P., B. Barnier, and A.P. de Miranda, A sigma-coordinate primitive equation model for studying the circulation in the South Atlantic, II, Meridional transports and seasonal variability, *Deep Sea Res., Part I*, 45, 573-608, 1998.
- Matano, R.P., and S.G.H. Philander, Heat and mass balances of the South Atlantic Ocean calculated from a numerical model, *J. Geophys. Res.*, 98, 977-984, 1993.
- McCartney, M.S., Subantarctic Mode Water, in *A Voyage of Discovery*, edited by M.V. Angel, pp. 103-119, Pergamon, Tarrytown N. Y., 1977.
- McCartney, M.S., The subtropical recirculation of Mode Waters, *J. Mar. Res.*, 40, supplement, 427-464, 1982.
- Pacanowski, R.C., K.W. Dixon, and A. Rosati, The GFDL Modular Ocean Model Users Guide, version 1.0, *GFDL Ocean Group Tech. Rep.* 2, 46 pp., Geophys. Fluid Dyn. Lab., Princeton, N.J., 1991.
- Peterson, R.G., and L. Stramma, Upper-level circulation in the South Atlantic Ocean, *Prog. Oceanogr.*, 26, 1-73, 1991.
- Peterson, R.G., and T. Whitworth III, The subantarctic and polar fronts in relation to deep water masses through the southwestern Atlantic, *J. Geophys. Res.*, 94, 10,817-10,838, 1989.
- Pickart, R.S., Water mass components of the North Atlantic Deep Western Boundary, *Deep Sea Res., Part A*, 39, 1553-1572, 1992.
- Poole, R., and M. Tomczak, Optimum multiparameter analysis of the water mass structure in the Atlantic Ocean thermocline, *Deep Sea Res. Part I*, in press, 1999.
- Provost, C., S. Gana, V. Garçon, K. Maamaatuaiahutapu, and M. England, Hydrographic conditions in the Brazil-Malvinas confluence during austral summer 1990, *J. Geophys. Res.*, 100, 10,655-10,678, 1995.
- Provost, C., C. Escoffier, K. Maamaatuaiahutapu, A. Kartavtseff, and V. Garçon, Subtropical mode waters in the South Atlantic Ocean, *J. Geophys. Res.*, this issue.
- Reid, J.L., On the total geostrophic circulation of the South Atlantic Ocean: Flow patterns, tracers and transports, *Prog. Oceanogr.*, 23, 149-244, 1989.
- Reid, J.L., On the total geostrophic circulation of the North Atlantic Ocean: Flow patterns, tracers and transports, *Prog. Oceanogr.*, 33, 1-92, 1994.
- Reid, J.L., On the circulation of the South Atlantic Ocean, in *The South Atlantic: Present and Past Circulation*, edited by G. Wefer et al., pp. 13-44, Springer-Verlag, New York, 1996.
- Rhein, M., L. Stramma, and U. Send, The Atlantic Deep Western Boundary Current: Water masses and transports near the equator, *J. Geophys. Res.*, 100, 2441-2457, 1995.
- Rhein, M., L. Stramma, and G. Krahnemann, The spreading of Antarctic bottom water in the tropical Atlantic, *Deep Sea Res., Part I*, 45, 507-527, 1998.
- Saunders, P.M., and B.A. King, Oceanic fluxes on the WOCE A11 section, *J. Phys. Oceanogr.*, 25, 1942-1958, 1995.
- Schott, F., L. Stramma, and J. Fischer, The warm water inflow into the western tropical Atlantic boundary regime, spring 1994, *J. Geophys. Res.*, 100, 24,745-24,760, 1995.
- Schott, F., J. Fischer, and L. Stramma, Transports and pathways of the upper-layer circulation in the western tropical Atlantic, *J. Phys. Oceanogr.*, 28, 1904-1928, 1998.
- Semtner, A.J., and R.M. Chervin, Ocean general circulation from a global eddy-resolving model, *J. Geophys. Res.*, 97, 5493-5550, 1992.
- Shannon, L.V., and G. Nelson, The Benguela: Large scale features and processes and system variability, in *The South Atlantic: Present and Past Circulation*, edited by G. Wefer et al., pp. 161-210, Springer-Verlag, New York, 1996.
- Siedler, G., T.J. Müller, R. Onken, M. Arhan, H. Mercier, B.A. King, and P.M. Saunders, The zonal WOCE sections in the South Atlantic, in *The South Atlantic: Present and Past Circulation*, edited by G. Wefer et al., pp. 83-104, Springer-Verlag, New York, 1996.
- Smythe-Wright, D., P. Chapman, C.D. Rae, L.V. Shannon, and S.M. Boswell, Characteristics of the South Atlantic subtropical frontal zone between 15°W and 5°E, *Deep Sea Res., Part I*, 45, 167-192, 1998.
- Speer, K.G., G. Siedler, and L. Talley, The Namib Col Current, *Deep Sea Res., Part I*, 42, 1933-1950, 1995.
- Speer, K.G., J. Holfort, T. Reynaud, and G. Siedler, South Atlantic heat transport at 11°S, in *The South Atlantic: Present and Past Circulation*, edited by G. Wefer et al., pp. 105-120, Springer-Verlag, New York, 1996.
- Stammer, D., R. Tokmakian, A.J. Semtner, and C. Wunsch, How well does a 1/4 degree global circulation model sim-

- ulate large-scale oceanic observations?, *J. Geophys. Res.*, **101**, 25,779-25,811, 1996.
- Stramma, L., and R.G. Peterson, The South Atlantic Current, *J. Phys. Oceanogr.*, **20**, 846-859, 1990.
- Stramma, L., and F. Schott, Western equatorial circulation and interhemispheric exchange, in *The Warmwatersphere of the North Atlantic Ocean*, edited by W. Krauss, pp. 195-227, Gebrüder Borntraeger, Berlin, 1996.
- Stramma, L., and F. Schott, The mean flow field of the tropical Atlantic Ocean, *Deep Sea Res., Part II*, **46**, 279-304, 1999.
- Stramma, L., J. Fischer, and J. Reppin, The North Brazil Undercurrent, *Deep Sea Res., Part I*, **42**, 773-795, 1995.
- Sverdrup, H.U., M.W. Johnson, and R.H. Fleming, *The Oceans: Their Physics, Chemistry and General Biology*, 1087 pp., Prentice-Hall, Englewoods Cliffs, N. J., 1942.
- Talley, L.D., Antarctic Intermediate Water in the South Atlantic, in *The South Atlantic: Present and Past Circulation*, edited by G. Wefer et al., pp. 219-238, Springer-Verlag, New York, 1996.
- Toggweiler, J.R., K. Dixon, and K. Bryan, Simulations of radiocarbon in a coarse-resolution world ocean model, I, Steady state prebomb distributions, *J. Geophys. Res.*, **94**, 8217-8242, 1989.
- Tokmakian, R., Comparisons of time series from two global models with tide-gauge data, *Geophys. Res. Lett.*, **23**, 3759-3762, 1996.
- Tomczak, M., and J.S. Godfrey, *Regional Oceanography: An Introduction*, 422 pp., Elsevier, New York, 1994.
- Tsuchiya, M., Thermohads and circulation in the upper layer of the Atlantic Ocean, *Prog. Oceanogr.*, **16**, 235-267, 1986.
- Tsuchiya, M., Circulation of the Antarctic Intermediate Water in the North Atlantic Ocean, *J. Mar. Res.*, **47**, 747-755, 1989.
- Tsuchiya, M., L.D. Talley, and M.S. McCartney, Water-mass distributions in the western South Atlantic; A section from South Georgia Island (54S) northward across the equator, *J. Mar. Res.*, **52**, 55-81, 1994.
- Warner, M.J., and R.F. Weiss, Chlorofluoromethanes in South Atlantic Antarctic Intermediate Water, *Deep Sea Res., Part A*, **39**, 2053-2075, 1992.
- Witter, D.L., and A.L. Gordon, Interannual variability of South Atlantic circulation from 4 years of TOPEX/POSEIDON satellite altimeter observations, *J. Geophys. Res.*, this issue.
- Wüst, G., Schichtung und Zirkulation des Atlantischen Ozeans. Die Stratosphäre des Atlantischen Ozeans, in *Wissenschaftliche Ergebnisse der Deutschen Atlantischen Expedition auf dem Forschungs- und Vermessungsschiff "Meteor" 1925-1927*, vol. 6, pp. 109-288, Walter de Gruyter, Berlin, 1935.

---

M. England, Centre for Environmental Modelling and Prediction, School of Mathematics, University of New South Wales, Sydney NSW 2052, Australia. (e-mail: matthew@maths.unsw.EDU.AU)

L. Stramma, Institut für Meereskunde Universität Kiel, Düsternbrooker Weg 20, 24105 Kiel, Germany. (e-mail: lstramma@ifm.uni-kiel.de)

(Received July 21, 1998; revised April 14, 1999; accepted April 28, 1999.)